รายงานวิจัยฉบับสมบูรณ์

โครงการ

การจำลองการปลูกฟิล์มบางแบบโมเลกุลาร์บีม เอพิแทกซีด้วยทฤษฎีกราฟ

โดย ผู้ช่วยศาสตราจารย์ ดร.สุรเชษฐ์ หลิมกำเนิด

กรกฎาคม 2557

สัญญาเลขที่ MRG5580245

รายงานวิจัยฉบับสมบูรณ์

โครงการ
การจำลองการปลูกฟิล์มบางแบบโมเลกุลาร์บีมเอพิแทกซี
ด้วยทฤษฎีกราฟ

ผู้ช่วยศาสตราจารย์ ดร. สุรเชษฐ์ หลิมกำเนิด
จุฬาลงกรณ์มหาวิทยาลัย

สนับสนุนโดยสำนักงานกองทุนสนับสนุนการวิจัย
(ความเห็นในรายงานนี้เป็นของผู้วิจัย สกว.ไม่จำเป็นต้องเห็นด้วยเสมอไป)

กิตติกรรมประกาศ

การทำงานที่มีความยุ่งยากแต่ละชิ้นให้สำเร็จลุล่วงอย่างมีคุณภาพจำเป็นต้องอาศัยความร่วมมือ ความชำนาญ และที่สำคัญที่สุด ความกรุณาจากหลายองค์กร หลายกลุ่มบุคคล จากหลายวาระโอกาส ดังต่อไปนี้

แนวคิดในการทำวิจัย จะไม่สามารถเปลี่ยนสภาพกลายเป็นผลงานวิจัยได้หากปราศจากเงินทุนสนับสนุน ข้าพเจ้าขอขอบพระคุณ **สำนักงานคณะกรรมการการอุดมศึกษา และสำนักงานกองทุนสนับสนุนการวิจัย** ที่ทำให้แนวคิดของข้าพเจ้ากลายเป็นความจริง

ข้าพเจ้าขอขอบพระคุณ **รองศาสตราจารย์ ดร. อุดมศิลป์ ปิ่นสุข** ที่ช่วยเหลือข้าพเจ้าในการดูแลภาพกว้างและให้คำปรึกษาในการทำวิจัย รวมถึงคอยชี้แนะเมื่อเกิดปัญหาและอุปสรรคระหว่างการทำงานอย่างไม่รู้จักเหน็ดเหนื่อย พร้อมทั้งคอยเตือนข้าพเจ้าให้เปลี่ยนมุมมอง และกระตุ้นให้เปลี่ยนโจทย์วิจัยเมื่อถึงทางตันอย่างทันท่วงที

งานวิจัยทางด้านการปลูกฟิล์มบางไม่ใช่งานที่ข้าพเจ้าจบกลับมาโดยตรง ข้าพเจ้าได้รับความช่วยเหลืออย่างดีจาก **ผู้ช่วยศาสตราจารย์ ดร. ปัจฉา ฉัตราภรณ์** ซึ่งเป็นผู้ที่คร่ำหวอดในการทำวิจัยทางด้านนี้มาอย่างโชกโชน อาจารย์ไม่รีรอที่จะยื่นมือเข้ามาช่วยให้คำปรึกษาและให้ความรู้แก่ข้าพเจ้าซึ่งยังใหม่ในวงการ และยิ้มรับคำถามพื้นฐานจากข้าพเจ้าอย่างไม่มีการเกี่ยงงอน

ข้าพเจ้าขอขอบพระคุณ ภาควิชาฟิสิกส์ และคณะวิทยาศาสตร์ จุฬาลงกรณ์มหาวิทยาลัย ที่เอื้อเฟื้อสถานที่ สาธารณูปโภคขั้นพื้นฐาน และคอมพิวเตอร์บางส่วนที่ใช้ในการจำลอง งานวิจัยชิ้นนี้จึงไม่อาจสัมฤทธิ์ผลได้หากขาดความอนุเคราะห์จากทางภาควิชา และท่านหัวหน้าภาค

และท้ายที่สุด ข้าพเจ้าขอขอบพระคุณ **ศูนย์วิจัยทางฟิสิกส์ของฟิล์มบาง (Research Center in Thin Film Physics)** ซึ่งเป็นส่วนหนึ่งของ**ศูนย์ความเป็นเลิศด้านฟิสิกส์ (Thailand Center of Excellence in Physics: ThEP)** ซึ่งเอื้อเฟื้องบประมาณ และคอมพิวเตอร์อีกส่วนหนึ่งสำหรับงานวิจัย นอกจากนี้ข้าพเจ้ายังได้รับความรู้มหาศาลจากการพูดคุยกับนักวิจัย และนิสิต นักศึกษาของศูนย์วิจัย สำหรับแนวคิดต่าง ๆ ที่เกิดขึ้น ซึ่งแนวคิดเหล่านี้ย่อมโยงใยและหลอมรวมกันไปสู่องค์ความรู้หลักของชิ้นงานอย่างแยกไม่ได้

Abstract

Project Code : MRG5580245

Project Title : Graph Theoretic Approach to Modeling Growth of Thin Films under Molecular Beam Epitaxy Technique

Investigator : Asst. Prof. Surachate Limkumnerd, Ph.D. Chulalongkorn University

E-mail Address : surachate.l@chula.ac.th

Project Period : July 2012 – July 2014

Interests in thin-film fabrication for industrial applications have driven both theoretical and computational aspects of modeling its growth. One of the earliest attempts toward understanding the morphological structure of a film's surface is through a class of solid-on-solid limited-mobility growth models such as Family, Wolf-Villain or Das Sarma-Tamborenea models which have produced fascinating surface roughening behaviors. These models however restrict the motion of an incidence atom to be within the neighborhood of its landing site which renders them inapt for simulating long-distance surface diffusion such as that observed in thin film growth using molecular-beam epitaxy (MBE) technique. Naive extension of these models by repeatedly applying the local diffusion rules for each hop to simulate large diffusion length can be computationally very costly when certain statistical aspects are demanded. We present a graph theoretic approach to simulating long-range diffusion-attachment growth model. Using Markovian assumption and given a local diffusion bias, we derive the transition probabilities for a random walker to traverse from one lattice site to the others after a large, possibly infinite, number of steps. Only computation with linear-time complexity is required for the surface morphology calculation without other probabilistic measures. The formalism is applied, as illustrations, to simulate surface growth on a two-dimensional flat substrate and around a screw dislocation under the modified Wolf-Villain diffusion rule. A rectangular spiral ridge is observed in the latter case with a smooth front feature similar to that obtained from simulations using the well-known multiple registration technique. An algorithm for computing the inverse of a class of sub-stochastic matrices is derived as a corollary.

Keywords : random walk, molecular-beam epitaxy, Markov process, graph theory

บทคัดย่อ

รหัสโครงการ : MRG5580245

ชื่อโครงการ : การจำลองการปลูกฟิล์มบางแบบโมเลกุลาร์บีมเอพิแทกซีด้วยทฤษฎีกราฟ

ชื่อนักวิจัย : ผู้ช่วยศาสตราจารย์ ดร. สุรเชษฐ์ หลิมกำเนิด จุฬาลงกรณ์มหาวิทยาลัย

E-mail Address : surachate.l@chula.ac.th

ระยะเวลาโครงการ : กรกฎาคม 2555 – กรกฎาคม 2557

ความสนใจเกี่ยวกับการผลิตฟิล์มบางเพื่องานประยุกต์ด้านอุตสาหกรรมเป็นตัวผลักดันงานวิจัยด้านทฤษฎีและด้านจำลองการปลูกฟิล์มบางในหลายปีที่ผ่านมา ความพยายามแรกในการทำความเข้าใจโครงสร้างของพื้นผิวฟิล์มกระทำผ่านแบบจำลองที่จำกัดระยะการเคลื่อนที่ของอะตอม เช่น แบบจำลองของแฟมิลี, วูล์ฟ-วิลเลน, และดาสซามา-ทามโบรินี ซึ่งให้โครงสร้างผลึกที่มีความขรุขระที่น่าสนใจเชิงสถิติ อย่างไรก็ตาม แบบจำลองเหล่านี้จำกัดระยะการเคลื่อนที่ของอะตอมให้อยู่เพียงตำแหน่งของพื้นผิวรอบจุดที่อะตอมตกเท่านั้น ทำให้แบบจำลองเหล่านี้ไม่สามารถแสดงลักษณะการเติบโตของผิวฟิล์มที่อะตอมสามารถเคลื่อนที่เป็นระยะทางไกลเช่นที่พบในการปลูกฟิล์มด้วยเทคนิคโมเลกุลาร์บีมเอพิแทกซีได้ ความพยายามในการขยายผลของงานจำลองแบบเดิมด้วยการทำการเคลื่อนที่ซ้ำหลาย ๆ ครั้งส่งผลให้เกิดความสิ้นเปลืองทรัพยากรในการคำนวณเป็นอย่างมาก อีกทั้งยังไม่สามารถให้ผลลัพธ์ที่มีคุณค่าทางสถิติเท่าที่ควร ในงานวิจัยชิ้นนี้ ผู้วิจัยได้ใช้ทฤษฎีกราฟในการจำลองการปลูกฟิล์มที่มีระยะการเคลื่อนที่ของอะตอมไกล ผู้วิจัยเริ่มจากสมมติฐานมาร์คอฟและกฎการเคลื่อนที่ของอะตอมระยะใกล้ในการคำนวณเมทริกซ์การส่งผ่านซึ่งให้ค่าความน่าจะเป็นที่อะตอมจะเคลื่อนที่ไปยังจุดที่สนใจบนผิวฟิล์มหากจำนวนก้าวกระโดดมีค่าสูง เราพบว่าอัลกอริทึมสำหรับคำนวณการเติบโตของผิวฟิล์มตามเวลามีความยุ่งยากที่แปรผันกับจำนวนตำแหน่งของอะตอมที่เป็นไปได้บนผิวฟิล์มเท่านั้น เราได้ใช้อัลกอริทึมใหม่นี้ในการจำลองการเติบโตของฟิล์มผิวเรียบในสองมิติ และการเติบโตของผิวฟิล์มรอบดิสโลเคชันแบบเกลียวภายใต้เงื่อนไขการแพร่แบบวูล์ฟ-วิลเลน เราพบลักษณะของเกลียวบันไดวนรูปสี่เหลี่ยมแบบเดียวกันกับที่พบในผลการจำลองแบบอื่นที่สิ้นเปลืองทรัพยากรในการคำนวณกว่า นอกจากนี้เรายังค้นพบการคำนวณเมทริกซ์ผกผันของเมทริกซ์จำพวกซับสโตแคสติคแบบหนึ่งอีกด้วย

คำหลัก : การเคลื่อนที่แบบสุ่ม, โมเลกุลาร์บีมเอพิแทกซี, กระบวนการมาร์คอฟ, ทฤษฎีกราฟ

Executive Summary

Due to the energy crisis looming the nation, research on alternative fuels is pivotal for the country's industrial and financial prosperity. Thin-film solar cells have shown great promises primarily for their relatively low production cost, endurance, and compatibility to Thailand's natural climate. Experimentation on thin-film solar cells, dating back a few decades ago, has sped up recently at the university level and in research institutions such as the Research Center in Thin Film Physics. To much dismay, theoretical and computational efforts on this subject have been lacking and thus are unable to provide fruitful and testable contributions to the experiment. Questions, such as what is an ideal condition for film of particular crystalline structure to grow smoothly or given an initial substrate profile what would be its eventual structure after growth, have never been thoroughly understood. Initial steps have been taken in trying to model thin film growth using molecular beam epitaxy technique using several toy models. These models, though easily implemented and recently modified to represent myriad lattice structures, fail to realistically recreate atomic behaviors at high enough temperature scales, where atoms diffuse for an appreciable distance, due to insufficient computational resource and naive algorithms. In this work the principle investigator proposes a novel approach to modelling epitaxially grown thin film. Using techniques in graph theory and stochastic processes, the method offers a new way to model long-range diffusion-attachment film growth together with growth's statistics. The study should be beneficial not only to solar cell fabrication but to other fields of thin film technology where surface properties are of considerable importance.

เนื้อหางานวิจัย

Contents

1 Introduction & Objectives

Limited mobility solid-on-solid diffusion models as means to study surface growth continue to attract much interest even after decades of investigations both computationally and analytically. In Wolf–Villain (WV) model [45], adatom moves in the direction that *maximizes* its coordination number in the next discrete time step; while in Das Sarma–Tamborenea (DT) model [14], it moves to *increase* the number provided that the current one is not sufficiently high. In both models, and others like them, adatom moves one lateral step before coming to a halt. Despite their simplicity, they are found to yield consistent simulation results with more realistic finite-temperature model using Arrhenius hopping rate [13, 40] and low-temperature MBE experiments [31]. These models, however, are inadequate as tools to investigate surface evolution in cases where each adatom undergoes a large number of hops before it

is embedded as part of the surface. The simplest extension these models to mimic a large diffusion length by repeated applications of one-step motion cannot avoid prescribing an ad-hoc maximum cutoff distance, and often is too computationally intensive for problems which require large-scale and/or long-time simulations. Furthermore this basic approach does not give any statistics of the growth in any straightforward way. A more systematic approach is needed. The aim of this paper is to present a graph-based method to model long-ranged solid-on-solid diffusion-attachment surface growth where, one at a time, an adatom is deposited onto a surface where each hop is determined by the local environment and is independent upon the previous ones. Our method can, in principle, provide statistics such as the average mean free path of growth particles and give the most probable surface pattern under any given lattice structure and local diffusion rule.

Graph theory has been at the core of mathematics and computer science and has recently fueled considerable interests in understanding the behaviors of complex networks [28, 39, 2, 7]. One of the theory's vast applications is in the development of random walks on graphs [25, 10] where a random walker traverses from one vertex to subsequent ones along (possibly weighted) edges connecting them. To use this idea to model surface growth on lattice due to long-range adatom diffusion, we construct a graph whose vertex i represents a lattice position and stores in it relevant lattice-dependent properties (such as atomic height at that point). An edge connecting two neighboring vertices i and k signifies a non-zero probability P_{ik} of an adatom, if present at i, would hop to k. This hop thus decreases the height value stored in i, and increases that stored in k by one unit. The weight of each edge can be obtained, as is the case here, from a chosen diffusion model such as WV or DT, or from a more realistic calculation using density functional theory. Through this graph, we establish the most likely final position of a deposited atom whose trip begins at i, and the average number of hops it takes to get there. By repeating this process, the surface is evolved.

To test our method, we choose to apply it to simulating the spiral surface growth around a screw dislocation commonly observed in MBE grown films with lattice mismatch at the film-substrate interface such as that of

GaN based devices [20, 32, 12], or certain semiconductor materials [38], and is known to provide a mechanism for driving the growth of a class of nanowires [27]. Unlike the spiral growth in the limit of fast desorption, where the ridge motion can be determined locally and is well described by Burton–Cabrera–Frank (BCF) model [8, 9], the minimal desorption limit where particle's diffusion length is comparable to the system size still presents a modeling challenge. Theoretical and computational investigations of spiral growth in this regime are typically carried out in a continuum limit using a phase-field method [34, 49]. This method although provides an analytical handle to the problem, it suffers from the shortcomings of a continuum formulation, e.g., when accounting for system's anisotropy. Kinetic Monte-Carlo (kMC) method has also been chosen to explore the spiral growth [48, 47]. In order to suppress microscopic noise, either the use of multiple-registration [46, 41] or atomic evaporation [48, 47] schemes must be implemented. The latter, though more realistic, is less practical at the extremely low supersaturation limit being considered.

2 Mathematical construct

The mathematical question underlying our modeling of particle diffusion with possibly infinite diffusion length amounts to finding the probability that a random walker beginning its journey at position i on a lattice would reach far-away point j by traveling along the edges connecting them. Edges linking, say, vertex i to its neighbors are not necessary of equal weights. Biased or asymmetric walks are accounted for by having directed weighted edges. This type of walks is required for modeling diffusion in the presence of fields such as in electromigration [4] or when adatoms sensitively react to local atomic configurations. The Markovian assumption that each step the walker takes is independent of the previous one was proven to be quite accurate [44]. If only nearest-neighbor hopping is allowed, only edges linking nearest neighbors are present and the graph structure matches the structure of the lattice surface. In principle one can incorporate long atomic jumps by including edges linking remote sites with a suitably weight factor. This type of jumps has been

observed experimentally with fairly significant jump rates [3, 29, 24]. For simplicity we shall only limit ourselves to one random walker. This allows us to easily define system's state at a given time by the lattice position of the walker. A more complicated scheme is required to define a state should one choose to model, e.g., clustered or collective diffusion [30].

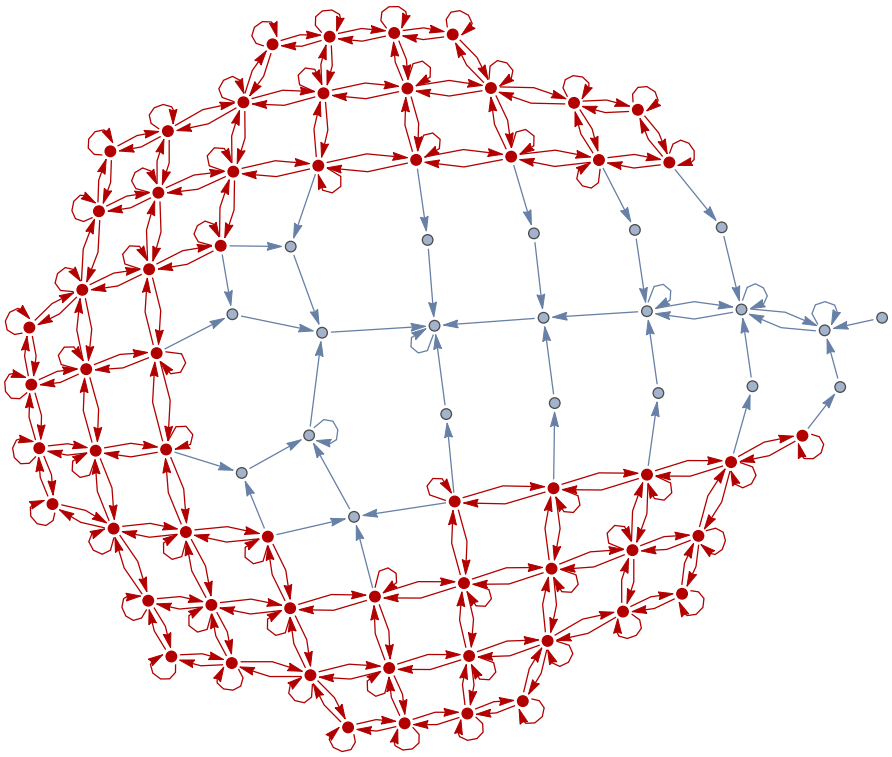

Figure 1: A graph representation of a transition matrix whose vertices symbolize states of the system in terms of adatom's position. Each arrow depicts an edge linking two positions whose transition probability from one to the other is non-zero. The probability is derived from WV diffusion rule on a circularly shaped substrate with a screw dislocation. One can see the trace of the underlying simple cubic lattice structure from the graph. Vertices and edges in red (dark gray) show a part of the graph which is strongly connected. These vertices form a class.

In this section, we shall outline the relevant portions of discrete time Markov chain needed for the modeling and state our graph algorithm for computing the infinite-hop transition matrix. For an illustrative purpose,

we shall phrase the problem in the language of crystal growth where an adatom wanders from point i to point j according to a given set of diffusion rules by hopping between atomic positions (vertices) linking i and j. Let a lattice configuration, some lattice-dependent property which influences the probability of the adatom such as atomic heights, be described by $\vec{H} \equiv \{H_i\}$. Define a one-step transition matrix $\mathbb{P}(\vec{H})$ whose element $P_{ik}(\vec{H})$ gives a transition probability for an atom at i to go to one of the connecting sites k which usually is a nearest neighboring lattice site. A non-zero element P_{ik} is thus equivalent to having a directed edge with a corresponding probabilistic weight connecting vertex i to vertex k of a graph as shown, for example, in Fig 1. We also account for in-place hopping through the matrix element P_{ii} (represented graphically by a vertex with self loop). Since the adatom must go somewhere $\sum_k P_{ik} = 1$ which makes $\mathbb{P}$ a stochastic matrix. Knowing $\mathbb{P}$, one can easily find the transition probability from i to j if the atom takes *exactly* n hops using

$$P_{ij}^{(n)} = \sum_k P_{ik} P_{kj}^{(n-1)} = \sum_{k_1,k_2,\ldots,k_{n-1}} P_{ik_1} \cdots P_{k_{n-1}j}\,, \tag{1}$$

or simply, $\mathbb{P}^{(n)} = \mathbb{P}^n$ in matrix notation. Since we are interested in the long diffusion limit, we shall investigate in particular the case where $n \to \infty$.

2.1 Lattice site classification

Given the state of height configuration $\vec{H}$, one can classify lattice position j (or system's state) according to the limiting behavior of $\mathbb{P}^\infty$ into *transient class* (denoted by $\mathcal{T}$) or *recurrent class* (denoted by $\mathcal{R}$). In case of finite number of system's states [18] (which is particularly relevant for modeling Markov processes on a computer), j is transient if $P_{ij}^\infty = 0$ and recurrent otherwise [1]. Loosely speaking, if one lets an adatom wander for a very long

[1] In particular these recurrent states are non-null. For $j \in \mathcal{R}$, it is non-null if $\mu_j \equiv \sum_{n=0}^\infty n F_{jj}^n$ is finite. Here F_{ij}^n is the first passage probability which denotes the likelihood that a walker starting at i will end up at j for the first time after exactly n hops. Thus μ_j gives mean recurrence time of state j or the expected value of the time of the first visit to j from j.

time, it will end up at one of the recurrent sites. It is easy to see that there must be at least one such site, otherwise $P_{ij}^{\infty} = 0$ for all j with edge(s) directed from i. This would lead to $\sum_j P_{ij}^{\infty} = 0$ and we would reach a contradiction because the adatom starting from i must go somewhere. The real merit of this classification is that it can be done through permuting rows and columns of $\mathbb{P}$ which amounts to relabeling of lattice positions, and prior to the actual computation of $\mathbb{P}^{\infty}$ itself.

If $\mathbb{P}$ is reducible, i.e., if there exists at least one transient site, then by definition one can find a non-unique permutation matrix $\mathbb{Q}_1$ that transforms $\mathbb{P}$ into a block triangular form such that $\mathbb{Q}_1^{\top} \cdot \mathbb{P} \cdot \mathbb{Q}_1 = \left(\begin{smallmatrix} \mathbb{X} & \mathbb{Y} \\ \mathbb{O} & \mathbb{Z} \end{smallmatrix}\right)$, where $\mathbb{X}$ and $\mathbb{Z}$ are square matrices, and $\mathbb{O}$ is a matrix with all elements being zero. If $\mathbb{X}$ and $\mathbb{Z}$ are reducible still, then we can apply another symmetric permutation to them. If during the process there exist rows with nonzero entries only in diagonal blocks, these rows can be permuted to the bottom of the modified transition matrix. Finally we shall arrive at the upper-triangular block form or the *canonical form for reducible matrices* [26] of a system via permutation matrix $\mathbb{Q}$ formed from the products of previous permutation matrices:

$$\widetilde{\mathbb{P}} = \mathbb{Q}^{\top} \cdot \mathbb{P} \cdot \mathbb{Q} = \begin{pmatrix} \widetilde{\mathbb{P}}_{\mathcal{T}\to\mathcal{T}} & \widetilde{\mathbb{P}}_{\mathcal{T}\to\mathcal{R}} \\ \mathbb{O} & \widetilde{\mathbb{P}}_{\mathcal{R}\to\mathcal{R}} \end{pmatrix}, \tag{2}$$

where

$$\widetilde{\mathbb{P}}_{\mathcal{T}\to\mathcal{T}} = \begin{pmatrix} \mathbb{T}_1 & \mathbb{T}_{1,2} & \cdots & \mathbb{T}_{1,t} \\ \mathbb{O} & \mathbb{T}_2 & \cdots & \mathbb{T}_{2,t} \\ \vdots & \ddots & \ddots & \vdots \\ \mathbb{O} & \cdots & \mathbb{O} & \mathbb{T}_t \end{pmatrix}, \tag{3}$$

$$\widetilde{\mathbb{P}}_{\mathcal{T}\to\mathcal{R}} = \begin{pmatrix} \mathbb{S}_{1,1} & \cdots & \mathbb{S}_{1,r} \\ \vdots & \ddots & \vdots \\ \mathbb{S}_{t,1} & \cdots & \mathbb{S}_{t,r} \end{pmatrix}, \widetilde{\mathbb{P}}_{\mathcal{R}\to\mathcal{R}} = \begin{pmatrix} \mathbb{R}_1 & & \mathbb{O} \\ & \ddots & \\ \mathbb{O} & & \mathbb{R}_r \end{pmatrix}.$$

Each diagonal block matrix $\mathbb{T}_1, \ldots, \mathbb{T}_t$ is either irreducible or $\mathbb{O}$ and $\mathbb{R}_1, \ldots, \mathbb{R}_r$ are irreducible and stochastic. In the language of graphs, the graph represen-

tation of matrix $\mathbb{A}$ is irreducible if there is a sequence of directed edges linking every pair of vertices together, i.e., the graph is *strongly connected*. As an example, the vertices and edges highlighted in red (dark gray) in Fig. 1 make up a subgraph which is strongly connected. Thus their transition matrix representation is irreducible.

Through the application of $\mathbb{Q}$, the newly ordered, one-step transition matrix $\widetilde{\mathbb{P}}$ shows the separations of lattice sites into t transient classes $\mathcal{T}_1, \ldots, \mathcal{T}_t$, and r recurrent classes $\mathcal{R}_1, \ldots, \mathcal{R}_r$. The form also effectively suggests from which transient classes is a site in a recurrent class *accessible* [2]. It is therefore of paramount importance to devise an algorithm to construct $\mathbb{Q}$. We shall postpone this discussion to Section 2.3.

2.2 Limiting lattice transitions

To arrive at the limiting transition probability matrix $\mathbb{P}^\infty$, one is interested in examining the possibility of transitions between elements in $\mathcal{T}$ and/or $\mathcal{R}$. We shall state without proofs these results [26], some of which are most evident from the structure of $\widetilde{\mathbb{P}}$ in Equations (2) and (3). The following transitions from i to j lead to vanishing probability, $P_{ij}^\infty = 0$: (a) $i, j \in \mathcal{T}$, (b) $i \in \mathcal{R}_1$ but $j \in \mathcal{R}_2$, and (c) $i \in \mathcal{R}$ and $j \in \mathcal{T}$. In other words, after a large number of hops, if a random walker beginning its trip from any of the transient classes, it will eventually go to a recurrent class. If, however, it already starts its journey in one of the recurrent classes, it will stay there forever. The remarkable theorem due to Oskar Perron and Georg Froebenius [33, 16] enables us to compute the limiting probability distribution of the latter case when it exists, and otherwise provides the fraction of time the walker spends on each site in the class.

When a random walker starts its trip within a recurrent class, say $\mathcal{R}_f$ with m members, whose transition matrix is given by $\mathbb{R}_f$, that the infinite-hop limit of the transition matrix $\mathbb{R}_f^\infty \equiv \lim_{n\to\infty} \mathbb{R}_f^n$ exists depends on the

[2] Mathematically speaking, site j is said to be accessible from i ($i \to j$) if there is a non-zero probability that, starting from i, the adatom will reach j at some future hop ($P_{ij}^{(n)} > 0$ for some $n \geq 0$). Sites i and j communicate with each other ($i \leftrightarrow j$) if and only if $i \to j$ and $j \to i$, which can happen only when both i and j belong to the same class.

periodicity of $\mathbb{R}_f$. Since $\mathbb{R}_f$ is irreducible, it is *aperiodic* if there is only one eigenvalue with modulus 1 and the limit exists, otherwise it is *periodic* and the limit does not exist. A good example of a periodic matrix is $\left(\begin{smallmatrix} 0 & 1 \\ 1 & 0 \end{smallmatrix}\right)$, where each self multiplication gives the result which fluctuates between itself and the identity matrix. Physically speaking, if a walker enters this class, its position at later times will oscillate between one of the two sites indefinitely. The period of this chain is therefore two. More generally the period coincides with the number of eigenvalues of modulus 1 [3]. Once in a class, the probability distribution of the walker's positions is not constant in time but continually progresses from subclass to subclass and eventually returns to the original distribution after going through all p subclasses. In practice classifying a recurrent class by its periodicity is simple; a non-negative irreducible matrix is aperiodic if there is at least one positive element along the diagonal [26].

When the limit exists,

$$\mathbb{R}_f^{\infty} = \mathbf{e}_f \boldsymbol{\pi}_f^{\top} = \begin{pmatrix} \pi_{f_1} & \pi_{f_2} & \cdots & \pi_{f_m} \\ \pi_{f_1} & \pi_{f_2} & \cdots & \pi_{f_m} \\ \vdots & \vdots & & \vdots \\ \pi_{f_1} & \pi_{f_2} & \cdots & \pi_{f_m} \end{pmatrix}, \tag{4}$$

where $\mathbf{e}_f$ is a vector whose elements are all 1, and $\boldsymbol{\pi}_f$ is a unique Perron vector satisfying $\mathbb{R}_f^{\top} \cdot \boldsymbol{\pi}_f = \boldsymbol{\pi}_f$, with all positive elements and properly normalized so that $\|\boldsymbol{\pi}_f\|_1 = 1$. This vector represents the distribution of probabilities that the walker will be at a particular site eventually. On the other hand, when $\mathbb{R}_f$ is periodic, $\mathbf{e}_f \boldsymbol{\pi}_f^{\top}$ in (4) is the solution to the Cesàro average, i.e.,

$$\mathbb{C}_f \equiv \lim_{n\to\infty} \frac{\mathbb{1} + \mathbb{R}_f + \mathbb{R}_f^2 + \ldots + \mathbb{R}_f^n}{n} = \mathbf{e}_f \boldsymbol{\pi}_f^{\top}. \tag{5}$$

Matrix element $[\mathbb{C}_f]_{ij}$ represents the portion of time that the walker hops onto j irrespectively of its starting position i. Henceforth, for the sake of theoretical discussion, whenever we examine infinite-hop probability within

[3] Alternatively one can find the period p from the characteristic equation of $\mathbb{R}_f$ without directly computing its eigenvalues. See Ref. [26] for proof.

a recurrent class, we shall adopt the Cesàro average interpretation in place of $\mathbb{R}_f^\infty$ when the latter does not exist.

The remaining question is to determine how probable it is for a walker to end up in one of the above recurrent classes if it starts from a transient class. Suppose the hop starts from a site in $\mathcal{T}_s$, the walker might have to visit subsequent intermediate transient classes $\mathcal{T}_m$'s, for all m connecting s to recurrent class $\mathcal{R}_f$. The total probability will ultimately involve how long the walker spends in each class as it traverses. Let matrix element $[\mathbb{M}_s]_{ij}$ denotes the expected total number of hops onto site $j \in \mathcal{T}_s$ given that the first hop starts at $i \in \mathcal{T}_s$, and $\mathbb{T}_s$ be the transition probability matrix among members in $\mathcal{T}_s$. Since the walker will either hop onto j with probability $[\mathbb{T}_s^n]_{ij}$ in which case the hop value is 1, or it won't which brings the hop value to 0. This means $[\mathbb{T}_s^n]_{ij}$ also represents the expected number of hop the walker will step onto j on the n^{th} step. Thus the total number of times the walker steps onto j on average is calculated from the total contributions from all steps:

$$\mathbb{M}_s = \sum_{n=0}^{\infty} \mathbb{T}_s = (\mathbb{1} - \mathbb{T}_s)^{-1} \tag{6}$$

The non-negativity and irreducibility of $\mathbb{T}_s$, and the fact that all of its eigenvalues have modulus strictly less than 1 ensure that the above Neumann series exists and is positive definite [26]. Matrix $\mathbb{1} - \mathbb{T}_s$ is an example of what's called *M-matrix*, and often emerges in relation to systems involving linear or nonlinear equations in many areas including solving finite difference methods, problems in operations research, and Markov processes [6].

Consider a transient class $\mathcal{T}_{s+1}$ which can be reached only from $\mathcal{T}_s$. The probability that a walker starting at site $i \in \mathcal{T}_s$ will wander to $j \in \mathcal{T}_{s+1}$ after an infinite number of hops must equal the expected period that the walker is going to spend on some site $k \in \mathcal{T}_s$ times the probability that it will exit $\mathcal{T}_s$ through k into $\mathcal{T}_{s+1}$, summing over all transitory sites k's:

$$\sum_{k \in \mathcal{T}_s} [\mathbb{M}_s]_{ik} [\mathbb{T}_{s,s+1}]_{kj} = [\mathbb{M}_s \cdot \mathbb{T}_{s,s+1}]_{ij} \tag{7}$$

It is easy to extend the result in (7) to the case where there are other intermediate transient classes and/or more than one route for the walker to take until it reaches some chosen transient class $\mathcal{T}_x$. Let $\mathbf{p} = \{p_1, \ldots, p_m\}$ be a path that connects transient class $\mathcal{T}_s$ to $\mathcal{T}_x$ via m intermediate classes $\mathcal{T}_{p_1}, \ldots, \mathcal{T}_{p_m}$. The exiting probability matrix is given by summing over the contributions from all such paths according to

$$\mathbb{P}^{\text{exit}}_{s,x} = \sum_{\mathbf{p}} \mathbb{M}_s \cdot \mathbb{T}_{s,p_1} \cdot \mathbb{M}_{p_1} \cdot \mathbb{T}_{p_1,p_2} \cdots \mathbb{M}_{p_m} \cdot \mathbb{T}_{p_m,x}. \tag{8}$$

Moreover the probability that the walker in $\mathcal{T}_x$ will transit to $\mathcal{R}_f$ is simply $\mathbb{M}_x \cdot \mathbb{S}_{x,f}$. Combining this result with (8), we finally arrive at the expression for the probability that a walker starting from a site in $\mathcal{T}_s$ will be entrapped in $\mathcal{R}_f$ after a large number of hops:

$$\mathbb{S}^{\infty}_{s,f} = \sum_{x} \mathbb{P}^{\text{exit}}_{s,x} \cdot \mathbb{M}_x \cdot \mathbb{S}_{x,f} \cdot \mathbb{R}^{\infty}_f \tag{9}$$

The sum $\sum_x$ is taken over all possible $\mathcal{T}_x$'s from which $\mathcal{R}_f$ can be accessible.

The result of this analysis can be summarized by the following matrix,

$$\widetilde{\mathbb{P}}^{\infty} = \begin{pmatrix} \mathbb{O} & \cdots & \mathbb{O} & \mathbb{S}^{\infty}_{1,1} & \cdots & \mathbb{S}^{\infty}_{1,r} \\ \vdots & \ddots & \vdots & \vdots & \ddots & \vdots \\ \mathbb{O} & \cdots & \mathbb{O} & \mathbb{S}^{\infty}_{t,1} & \cdots & \mathbb{S}^{\infty}_{t,r} \\ \mathbb{O} & \cdots & \mathbb{O} & \mathbb{R}^{\infty}_1 & & \mathbb{O} \\ \vdots & \ddots & \vdots & & \ddots & \\ \mathbb{O} & \cdots & \mathbb{O} & \mathbb{O} & & \mathbb{R}^{\infty}_r \end{pmatrix}, \tag{10}$$

together with $\mathbb{S}^{\infty}_{s,f}$ as defined in (9), and $\mathbb{R}^{\infty}_f$ as in (4) with the appropriate limit interpretation. Given initial state vector $\mathbf{v}_i$, after a large number of hops, the system's probability distribution is therefore

$$\mathbf{v}_f = \mathbf{v}_i \cdot \widetilde{\mathbb{P}}^{\infty}. \tag{11}$$

2.3 Graph algorithms

The analysis so far has made full use of the canonical form for reducible matrices. The question thus arises: is there a way to systematically find a permutation which would cast a reducible matrix into its canonical form? Fortunately in graph theory there exists a set of algorithms which does exactly this. Initially one can find a permutation which could swap indices in such a way that strongly connected components (or lattice sites in this case) are grouped together into appropriate classes. Algorithms such as Tarjan's and Gabow's exist to do this with linear-time complexity [5, 11]. At this point, the relationship between classes can be represented by a non-unique *Directed Acyclic Graph* (DAG).

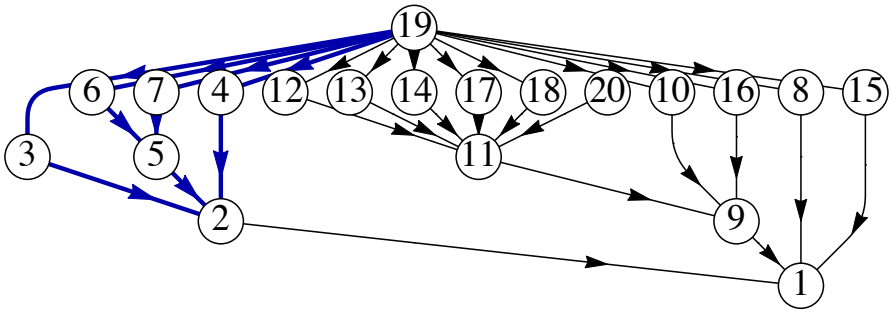

Figure 2: The directed acyclic graph (DAG) of the graph shown in Fig. 1. Each vertex represents a class of strongly connected components, and each edge connects two classes with non-vanishing transition probability from one to the other. Vertex 19, for example, represents the subgraph in Fig. 1 that is highlighted in red (dark gray).

Let $G = (V, E)$ be a DAG with a set of vertices $V = \{1, 2, \ldots, t + r\}$ and a set of edges E. Vertex i represents a transition matrix of type (a) $\mathbb{T}_i$ for all i whose outdegree is positive ($\deg^+(i) > 0$); or (b) $\mathbb{R}_i$ if i is a *sink* ($\deg^+(i) = 0$). The underlying graphs of these matrices are, by construction, strongly connected which make them irreducible. Edge (i, j) connecting vertex i to j represents transition matrix of type (a) $\mathbb{T}_{i,j}$ from $\mathcal{T}_i$ to $\mathcal{T}_j$ if $\deg^+(j) > 0$; or (b) $\mathbb{S}_{i,j}$ from $\mathcal{T}_i$ to $\mathcal{R}_j$ if j is a sink. An example of such a graph is

shown in Fig. 2. Vertices in a DAG have a natural ordering which could best be visualized by a layered tree, pointing one way from vertices of transient classes to those of recurrent classes. A *topological sorting* [22, 42] can be performed in linear time ($\mathcal{O}(|V| + |E|)$) to yield a permutation of classes from transient to recurrent. By composing the two permutations together, one obtains a permutation which takes a reducible matrix to its canonical form. In practice it is not important to topologically sort DAG to obtain the full canonical form to efficiently compute elements of $\widetilde{\mathbb{P}}^{\infty}$. The ordering of $\mathbb{M}_a \cdot \mathbb{T}_{a,b}$ terms in Equation (7) only requires that they appear in the same sequence as the underlying DAG. Topological sorting simply relabels the class numbers in order of appearance which yields no new information, and thus is unnecessary.

In cases where a prescribed diffusion rule prohibits self hopping ($P_{ii} \neq 0, \forall i$), the limiting probability transition may not exist for some recurrent class $\mathcal{R}_i$. If preferred, one can determine the period of $\mathcal{R}_i$ directly from its underlying subgraph G^i. From graph theoretic perspective, G^i is periodic with period p if and only if it can be partitioned into p smaller graphs $G^i_1, \ldots, G^i_p$ such that (a) if vertex m is in G^i_k and an edge (m, n) connects m to n then it's implied that n is in $G^i_{(k+1) \bmod p}$; and (b) p is the largest possible integer with this property. This makes sure that each transition takes the walker to a new class before it returns to the original class after p successive transitions. An aperiodic recurrent class is one where such partition is not possible. The proof of the above theorem and the graph algorithm for finding the period of these "cyclically moving classes" are given in Ref. [21].

To employ G in the limiting probability calculation, we start by assigning appropriate matrices to all vertices and edges. Let $S = \{j | \deg^+(j) = 0\}$ be the set of all sinks of G. We then assign matrix $\mathbb{M}_i$ to each vertex $i \notin S$, or $\mathbb{R}^{\infty}_i$ for $i \in S$. Each edge (i, j) is prescribed by transition matrix $\mathbb{T}_{i,j}$ for $j \notin S$, and $\mathbb{S}_{i,j}$ for $j \in S$. To compute the limiting probability that a walker would reach a site in one of the recurrent classes in S, we begin by giving the walker his initial probability distribution vector $\mathbf{v}_0$ at the starting class. This vector contains only one non-zero component of value 1 at the position corresponding to the dropped site. Then we scan the graph from the starting

vertex (which may or may not be the source) to the sinks. As we traverse the graph to vertex s, we would have accrued all the probability contributions along that path prior to reaching s. The probability distribution $\mathbf{v}_s$ stored at each vertex as it's visited would be

$$\mathbf{v}_s = \begin{cases} \sum_r \mathbf{v}_r \cdot \mathbb{M}_r \cdot \mathbb{T}_{r,s} & \text{if } s \notin S, \\ \left(\sum_r \mathbf{v}_r \cdot \mathbb{M}_r \cdot \mathbb{S}_{r,s} \right) \cdot \mathbb{R}_s^{\infty} & \text{if } s \in S. \end{cases} \tag{12}$$

The above summation $\sum_r$ is taken over all incoming vertices r that point toward s. In a special case where the graph is made up of just one vertex, the final distribution is simply the Perron vector $\boldsymbol{\pi}_s$. It should be emphasized that direct computations of all the $\mathbb{M}_s$ are not necessary. One only needs to calculate $\mathbf{x} \equiv \mathbf{v}_r \cdot \mathbb{M}_r$ which is equivalent to solving the system of linear equations of the form $(\mathbb{1} - \mathbb{T}_r^{\top}) \cdot \mathbf{x} = \mathbf{v}_r$. There exists many iterative schemes to determine $\mathbf{x}$ such as Jacobi method and successive over-relaxation (SOR) method [6, 43], or one could solve them using the equivalent constrained minimization method. As an illustration, according to the highlighted subgraph of G as shown in Fig. 2 (thick arrows), vertex 2 would receive probability vector $\mathbf{v}_2$ whose value equals

$$\begin{aligned} \mathbf{v}_2 = \mathbf{v}_{19} \cdot \mathbb{M}_{19} \cdot \Big[& \mathbb{T}_{19,3} \cdot \mathbb{M}_3 \cdot \mathbb{T}_{3,2} + \mathbb{T}_{19,4} \cdot \mathbb{M}_4 \cdot \mathbb{T}_{4,2} \\ & + \left(\mathbb{T}_{19,6} \cdot \mathbb{M}_6 \cdot \mathbb{T}_{6,5} + \mathbb{T}_{19,7} \cdot \mathbb{M}_7 \cdot \mathbb{T}_{7,5} \right) \cdot \mathbb{M}_5 \cdot \mathbb{T}_{5,2} \Big]. \end{aligned}$$

Vector $\mathbf{v}_2$ can be interpreted as the probability that a walker would reach each site in transient class $\mathcal{T}_2$ given its initial probability distribution of $\mathbf{v}_{19}$ in class $\mathcal{T}_{19}$. By the time sink 1 is reached, the limiting probability distribution vector $\mathbf{v}_1$ can readily be obtained from the $\mathbf{v}_r$'s of its immediate predecessors:

$$\begin{aligned} \mathbf{v}_1 = \Big[& \mathbf{v}_2 \cdot \mathbb{M}_2 \cdot \mathbb{S}_{2,1} + \mathbf{v}_8 \cdot \mathbb{M}_8 \cdot \mathbb{S}_{8,1} \\ & + \mathbf{v}_9 \cdot \mathbb{M}_9 \cdot \mathbb{S}_{9,1} + \mathbf{v}_{15} \cdot \mathbb{M}_{15} \cdot \mathbb{S}_{15,1} \Big] \cdot \mathbb{R}_1^{\infty} \end{aligned}$$

Other aspects of graph algorithm will be discussed in the respective sections as we examine the modeling problems. Reader interested in seeing the connection between DAG and the matrix inversion of the form $(\mathbb{1} - \mathbb{A})^{-1}$ where $\mathbb{A}$ is sub-stochastic should take a look in Appendix A.

3 Modeling

The formalism outlined in the previous section shall be applied to simulate long-range diffusion-attachment solid-on-solid growth on a two-dimensional substrate. For simplicity, the underlying lattice structure is simple cubic—though other crystalline structures are of no fundamental differences. Two examples shall be considered: (1) growth on an initially flat substrate, and (2) growth around a screw dislocation. For each initial profile of the substrate, graph g, similar to what's shown in Fig. 1, is constructed where a vertex represents a lattice position and an edge links a pair of adjacent neighbors together. Each vertex contains a number representing the height of the stack of atoms at that site. This implies that overhangs and voids are prohibited. An edge (i, k) contains probability P_{ik} that if an atom is deposited at i, it would move to k. For illustrative purposes, Wolf–Villain diffusion model is chosen to prescribe such weight. According to the model [45], an adatom will try to move in such a way that the lateral coordination number is maximized. Should there be more than one such directions, the probability is divided equally among them. A slight alteration is made to the rule by including the coordination number at the present position into consideration so that in-place hopping is possible ($P_{ii} \neq 0$). This modification permits the limiting transition probability $\mathbb{R}_s^\infty$ to always exist in our analyses. The underlying graph g of the transition matrix $\mathbb{P}$ serves as the starting point of all of our simulations. We shall examine the surface growth evolution of the examples when each incidence atom, one at a time, performs a random walk on the surface where the direction of each step is given by the modified WV model until the atom becomes a part of the surface. The final resting position of the atom is chosen from one where the atom has visited most frequently.

Before we discuss problem-specific modelings, it is a good idea to consider

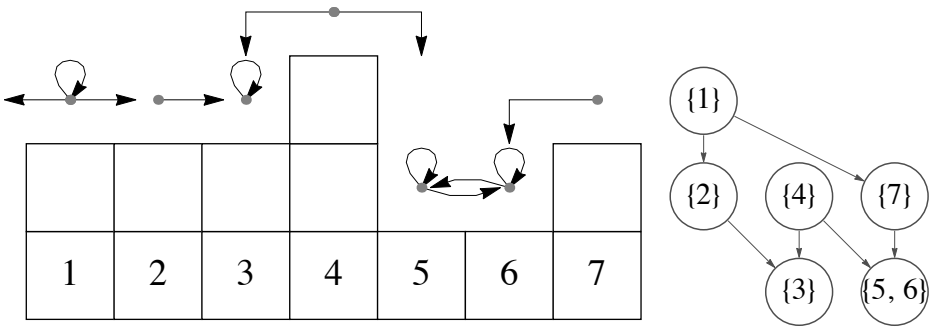

Figure 3: Diffusion rule for the modified Wolf–Villain model is shown on a sample of a one-dimensional substrate with periodic boundary conditions together with the associated directed acyclic graph. Atoms are deposited from the top and can move at most one step to the side. The arrows depict possible hop directions given the incidence positions. The self-looping arrows designate hopping in-place which is added in this modified version.

a simple example. Fig. 3 shows the side view of a one-dimensional lattice with periodic boundary conditions at an instant in time. According to our modified Wolf–Villain model, the arrow(s) on top of each surface position indicate possible directions that an atom, if dropped there, would move with the probability inversely proportional to the number of arrows at that point. Lattice positions are labeled by the numbers at the base. The one-step transition matrix is given by

$$\mathbb{P} = \begin{pmatrix} 1/3 & 1/3 & 0 & 0 & 0 & 0 & 1/3 \\ 0 & 0 & 1 & 0 & 0 & 0 & 0 \\ 0 & 0 & 1 & 0 & 0 & 0 & 0 \\ 0 & 0 & 1/2 & 0 & 1/2 & 0 & 0 \\ 0 & 0 & 0 & 0 & 1/2 & 1/2 & 0 \\ 0 & 0 & 0 & 0 & 1/2 & 1/2 & 0 \\ 0 & 0 & 0 & 0 & 0 & 1 & 0 \end{pmatrix}.$$

This example is simple enough that there is no need to cast $\mathbb{P}$ into its canonical form. It is clear from the structure of the matrix that the transient classes are $\{1\}, \{2\}, \{4\}$ and $\{7\}$, and the recurrent classes are $\{3\}$ and $\{5, 6\}$ (which are also our sinks). Since each transient class only contains one mem-

ber, matrix $\mathbb{M}_s$ is extremely simple; $\mathbb{M}_s = 1/(1 - P_{s,s})$ for $s \in \{1, 2, 4, 7\}$. The recurrent matrices are $\mathbb{R}_1^\infty = \{1\}$, and $\mathbb{R}_{\{5,6\}}^\infty = \left(\begin{smallmatrix} 1/2 & 1/2 \\ 1/2 & 1/2 \end{smallmatrix}\right)$. Matrices $\mathbb{P}_{s,x}^{\text{exit}}$ and $\mathbb{S}_{s,f}^\infty$ can be calculated from Equations (8) and (9) with the help of the DAG shown in Fig. 3. For example given that an atom starts its trip at site 1, the probability $\mathbb{P}_{1,3}^\infty$ that it will end up at site 3 can be computed in the following way:

$$\begin{aligned} \mathbb{P}_{1,3}^\infty = \mathbb{S}_{1,3}^\infty &= \mathbb{P}_{1,2}^{\text{exit}} \cdot \mathbb{M}_2 \cdot \mathbb{P}_{2,3} \cdot \mathbb{R}_3^\infty \\ &= (\mathbb{M}_1 \cdot \mathbb{P}_{1,2}) \cdot \mathbb{M}_2 \cdot \mathbb{P}_{2,3} \cdot \mathbb{R}_3^\infty \\ &= \left(\frac{1}{1 - \frac{1}{3}} \times \frac{1}{3} \right) \frac{1}{1 - 0} \times 1 \times 1 = \frac{1}{2} \end{aligned}$$

The resulting limiting transition probability matrix for this initial configuration is given by

$$\mathbb{P}^\infty = \begin{pmatrix} 0 & 0 & 1/2 & 0 & 1/4 & 1/4 & 0 \\ 0 & 0 & 1 & 0 & 0 & 0 & 0 \\ 0 & 0 & 1 & 0 & 0 & 0 & 0 \\ 0 & 0 & 1/2 & 0 & 1/4 & 1/4 & 0 \\ 0 & 0 & 0 & 0 & 1/2 & 1/2 & 0 \\ 0 & 0 & 0 & 0 & 1/2 & 1/2 & 0 \\ 0 & 0 & 0 & 0 & 1/2 & 1/2 & 0 \end{pmatrix}.$$

According to $\mathbb{P}^\infty$, an atom falling onto site i will eventually end up at site 3, 5 or 6 with probabilities as listed on the i^{th} row if one applies the modified WV rule repeatedly. Moreover, provided that an atom is likely to fall anywhere, site 3 is the most likely eventual resting place (because the third column of this matrix yields the largest sum) with the probability of 3/7.

Let us examine the structure of the sinks obtained from the modified WV model in a general two-dimensional substrate. Most of the time, a sink (recurrent) class only contains one member (like site 3 in our simple example above). This member is the representation of a kink site. Thus the task of computing Perron vectors to represent the $\mathbb{R}_s^\infty$ matrices is removed. Essentially these matrices are simply $\{1\}$. In a few rare cases we could have a

situation where two (site 5 and 6 in the above example), three or four kinks facing each other creating an area of two to four sites whose coordination numbers equal one another, and are higher than those of their surrounding neighbors'. Each vertex within a class with two (four) elements has two (three) edges, one pointing to itself and the rest point(s) to its neighbor(s). The limiting recurrent matrix $\mathbb{R}_s^\infty$ in this case would be a 2×2 (4×4) matrix with all elements being 1/2 (1/4). In the case of three elements, there is one vertex with three outgoing edges, while the other two only contain two edges. The Perron vector used in Eq. (4) comprises two of 2/7 and one of 3/7. Only in this last case is the weight not distributed evenly and the walker would more likely go there. Fortunately these cases never crop up in the analyses of the two-dimensional problems considered below.

3.1 Growth on flat substrate

Here we consider the surface growth on an initially flat rectangular surface with the periodic boundary conditions, and apply the algorithm discussed in the previous section to find the most likely site that each atom would likely be. Two different methods shall be used: (I) each deposition site is chosen randomly and the algorithm gives its most probable final position; and (II) the most probable final position of all initial sites shall be chosen. Notice that the first atom to be dropped onto the surface will as likely be at any one site as another. Thus, for a visual purpose, we put it at the center of the surface. This atom will act as the seed to which subsequent atoms can attach themselves in the process of island formation.

In Method I, for each iteration, the simulation scheme starts by randomly selecting a starting position i_0. Then only the subgraph of g whose components can be reached from i_0 is extracted. This process helps keep only the relevant irreducible classes for future computations. Subsequently the DAG G of this subgraph is constructed by grouping strongly connected components together. We choose the eventual resting position by looking for j which yields the greatest $P_{i_0 j}^\infty$. From the structure of G, one of three things could happen: (a) there is only one class thus G is the sink; (b) G only con-

tains one sink and j will inevitably be in that sink; or (c) G contains multiple sinks and further calculation needs to determine the most likely sink that j would eventually lie. It is only this last case that an actual calculation in the form outlined in Sec. 2.3 is performed if all one wishes is to get the final position of the adatom without calculating any statistics. Once all $\mathbf{v}_s, \forall s \in S$ are obtained, the chosen sink is the one whose member has the greatest value among all elements in all sink classes. Should there be more than one such members, the chosen site is selected randomly from that list. We then increment the atomic height at that site by one unit and the whole routine is repeated. Method II is similar to Method I except for one important point; our initial probability distribution $\mathbf{v}_i$ is given by $(1/N)\{1, \ldots, 1\}$, instead of having one non-zero element at a random position i_0.

3.2 Growth around a screw dislocation

In modeling the surface growth around a screw dislocation, we decide upon a circularly shaped substrate of radius r with free boundary. This choice ensures that any rectangular pattern that might emerge from the growth is due to the underlying lattice structure and not due to the shape of the boundary. Sites along the rim of the disk only connects with those within; thus they contain less nearest neighbors than the ones within the disk. The total number of lattice positions is approximately πr^2. We first initialize the height of all lattice points according to $h(x, y) = (b/2\pi)\tan^{-1}(y/x)$. Traversing around the dislocation core at $(0, 0)$ once in the clockwise (counter-clockwise) direction will result in a height increment (decrement) approaching b at large distance from the core. In order to specify the coordination number at each point on the lattice, one needs to specify the criterion for height difference between any adjacent sites. If the height difference between two nearest-neighboring sites is smaller than $0.2b$, we consider them as living on the same plane, and an adatom on top of the shorter site will not receive the coordination number count from the taller one. The simulation procedures in this case are the same as that of the flat surface. After the most probable site is found in either Method I or Method II, we increase its height by b to match the

magnitude of the Burgers vector. Then the process is repeated.

4 Results and discussions

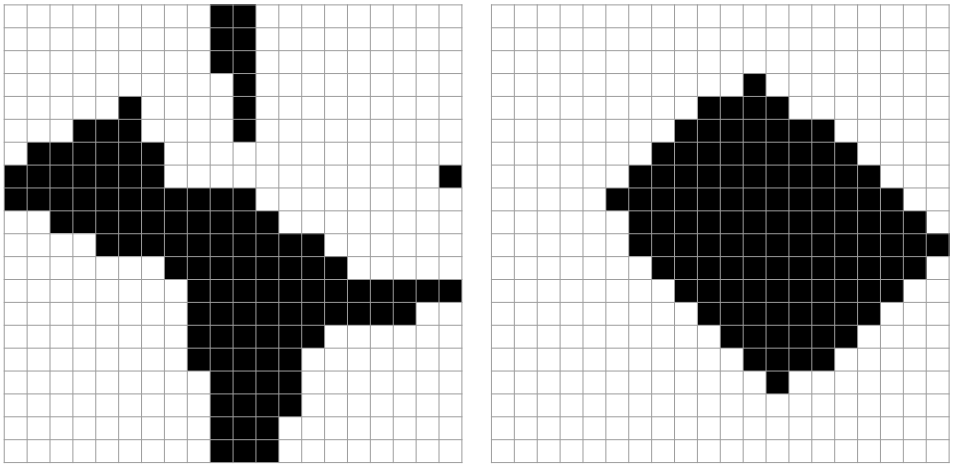

(a) (b)

Figure 4: Surface of size 20×20 lattice sites with periodic boundary conditions after 113 atoms (black squares) are deposited using (a) Method I, and (b) Method II.

The evolution in the case of growth on a flat substrate gives rise to one-island formation. In Method I, subsequent atoms attach themselves to the initial single-atom island since this is the only place where they can maximize their coordination number. The most probable final position of each newly deposited atom given by our algorithm tends to be the kink site that is closest to the dropped position. This results in an island surface with jagged island boundary as shown in Fig. 4 (a). The island will continue to grow until the first layer is completely filled up. This happens because there is no mechanism, e.g., Ehrlich–Schwoebel-like barrier, to prevent an adatom dropped on top of the island from hopping down to a lower layer where it could increase its coordination number. After the complete first layer is filled, the growth process repeats itself again and again, giving us a perfect layer-by-layer growth.

In Method II, the growth of the freshly deposited layer is largely symmetrical. Identifying the plane of the substrate to be (001), atoms collectively tend to form an island whose boundaries grow outward in a rectangular fashion with growth fronts perpendicular to the [110], [1$\bar{1}$0], [$\bar{1}$10] and [$\bar{1}\bar{1}$0] directions as can be seen in Fig. 4 (b). Unlike the previous case, the shape of the island is generally very compact. The development of the growth fronts can be observed since the early stage in the simulation. These orientations are favorable to incoming adatoms than others since they provide more lateral kink sites which result in higher coordination numbers than if the front were one of [100], [010], [$\bar{1}$00] or [0$\bar{1}$0]. As in the previous method, the surface is filled up one layer at a time.

The simulation result of the surface growth around a screw dislocation shows a more interesting dynamics. We initially align the ridge so that it extends radially outward from the dislocation core at $(0, 0)$ along the [0$\bar{1}$0] direction. When viewed from the top, the ridge starts spiraling outward in the clockwise direction (since the atomic height difference is $h(x = 0^+) - h(x = 0^-) = +b$ along the ridge) as more and more atoms are attracted toward its left side. The surface evolution according to Method I, like the flat substrate case, gives a very rough spiral ridge. The randomness of each deposition causes the atomic incorporation to occur at the nearest kink site which may be anywhere. This makes it difficult to describe how the surface grows generally. More importantly, the growth does not reflect the shape observed in actual experiments where the spiral ridge fronts are of well-defined compact geometrical form [20, 32, 12].

Result from Method II, on the other hand, does not suffer from this setback. During its first revolution, whose development is depicted in Fig. 5 (b) and (c), the spiral ridge looks like a four-pointed star whose boundary is concave. These concave fronts are filled up quickly afterward into straight edges orienting along the preferred directions making the spiral rectangular in appearance. The growth fonts are exactly the same as those seen in the case of flat substrate growth. As time progresses, more and more steps are generated and the surface looks like a rectangular pyramid. The distance between adjacent steps also decreases with time, as is typical seen in actual

growth experiment [17, 38] and also in the phase-field simulation [23]. With this particular boundary condition, we observe the stationary state when the width of successive steps is exactly one. Since the details of the growth evolution depend largely on the chosen diffusion rule (the modified WV in this case) and the boundary conditions, we shall postpone the full analyses of the dependence of surface growth on these choices for our future work.

It should be mentioned that the strange initial 'side-branching' spiral has never been observed elsewhere, either in the phase-field modeling or in energetic-based kMC simulations of growth around a dislocation. We believe that this artifact is specific to our choice of diffusion rule. The shape, however, is similar to a two-dimensional kMC growth simulation around a nucleation site with atoms having a short average mean free path [48]. By employing a multiple registration scheme, the island boundary was smoothed out and the dendritic feature with four side branches could be seen. We believe that their striking resemblance albeit different physical processes may not be a coincidence but an implication about a connection between our probabilistic approach and the approach using short-distance diffusion with multiple registration scheme [4]. As a noise reduction technique, the scheme allows for a more probable site to be chosen since atom must visit a site repeatedly up to a certain number before it becomes a part of the surface. Thus to some degree, the two approaches are similar. Further investigation is needed in order to quantify this connection.

As a demonstration of our probabilistic approach, Fig. 6 shows the mean free path λ, or the average number of hops an atom makes until its incorporation to the most likely spot on the spiral ridge, computed through Method I. The simulations were performed on the substrate of radius $r = 10$, 15 and 20 atomic spacings bringing the total number of sites to $N = 316$, 716 and 1264 respectively. About $6N$ atoms were sequentially dropped in each case. Points on the graph are the results of the average over 800, 400 and 300 runs respectively. All three graphs are more or less on top of one another except for the tail of the $r = 10$ case. Due to its small size, the system reaches its

[4]The latter was recently shown to be equivalent, and could provide an alternative approach to, simulating collective diffusion phenomenon on thin film growth [1].

stationary state long before the other two cases. The very first atom has to hop on the order of $N \sim r^2$ before it reaches the dislocation ridge. The number of hops decreases very rapidly as the ridge starts to spiral. We notice a series of plateaus starting approximately at every N^{th} atoms. A drop in the number of hops to the next plateau occurs as one or more of the ridge fronts are filled up and straightened out. Inside of a plateau region, new atoms take on average the same number of hops before reaching the spiral as its fronts propagate outward. This process continues until the stationary state is reached at which point atoms most likely would take at most a few hops before being incorporated into the spiral ridge. As points of reference, we include the shapes of the substrate, simulated by Method II, after N^{th}, $2N^{\text{th}}$, ..., $6N^{\text{th}}$ atoms are absorbed into the spiral.

A few remarks are in order before we end this section. In principle it is possible to obtain Fig. 6 using the conventional approach by directly applying the WV diffusion rule to each step until an atom no longer moves, while recording its hop number. Doing so repeatedly in order to achieve the same statistics presented here, however, would be computationally very costly. We were able to produce the data used to create the above graphs using about four days of computer time on a single core processor. If one is not interested in carrying out any statistical computations and only wants the evolution of the height profile, a much larger system can be simulated within a reasonable time. As mentioned earlier, in most cases the eventual resting site for each deposited atom may be obtained with minimal computation by simply looking at the structure of the underlying DAG. Finally, the technique presented in this work deals primarily with statistics of random walk on lattices given a local diffusion rule. Readers interested in practical tools for simulating thin film growth on an actual physical system should look into many recent developments aimed toward improving efficiency and accuracy of the conventional kMC algorithm. Amar et al. make use of clever parallel programming techniques to extend kMC over larger length and time scales [35], and are able to achieve simulation time that scales as, not the usual polynomial, but the logarithm of system size [36]. For a smaller system that demands full trajectories of deposited atoms, molecular dynamics (MD)

is generally utilized. Several accelerated dynamics algorithms have been proposed to speed up direct integrations of Newton's equations, more notably using temperature-accelerated MD technique [37]. Other attempts such as one that tries to approximate the MD methods to be used in conjunction with kMC calculations have also shown impressive speed improvement on long-time/large-scale systems over the conventional kMC approach [19]. Readers wishing to see theoretical basis submolonolayer growth kinetics and follow recent developments in cluster growth on surfaces should consult Ref. [15] and references therein.

5 Conclusion

Based on Markovian hypothesis and Froebenius theorem, the limiting probability transition matrix for a random walker starting his trip with a given initial probability profile is obtained. We devised graph algorithms to automate the process so that it could be implemented on a computer. In the process, we discover an algorithm for finding the inverse of a certain class of stochastic matrices. Finally the formalism is applied to solid-on-solid, diffusion-attachment type of surface growth on a two-dimensional flat substrate and around a screw dislocation. The latter gives a usual spiral ridge with rectangular shape reflecting the underlying crystal structure in the limit where atoms are set to emerge at the most probable lattice positions during growth. The result also suggests an interesting connection with the widely-used multiple registration technique in kMC simulations.

A DAG and matrix inversion

An algorithm such as that of Tarjan's which casts a matrix into the corresponding directed acyclic graph from where permutation matrix $\mathbb{Q}$ could be constructed, offers a new way of computing an inverse of a certain class of matrix. It is well known that the inverse of a triangular block matrix is given

by

$$\begin{pmatrix} \mathbb{B}_1 & \mathbb{B}_2 \\ \mathbb{O} & \mathbb{B}_3 \end{pmatrix}^{-1} = \begin{pmatrix} \mathbb{B}_1^{-1} & -\mathbb{B}_1^{-1} \cdot \mathbb{B}_2 \cdot \mathbb{B}_3^{-1} \\ \mathbb{O} & \mathbb{B}_3^{-1} \end{pmatrix}. \tag{13}$$

We shall use Eq. (13) as a basis for our analysis.

We are interested in finding the inverse of matrix $\mathbb{D} \equiv \mathbb{1} - \mathbb{A}$ where $\mathbb{A}$ is a sub-stochastic matrix whose summation of elements in each row is less than or equal to 1. We start by obtaining $\mathbb{Q}$ through Tarjan's algorithm. Matrix $\mathbb{Q}$ can be used to turn $\mathbb{A}$, through a simple change-of-basis, into

$$\widetilde{\mathbb{A}} \equiv \mathbb{Q}^\top \cdot \mathbb{A} \cdot \mathbb{Q} = \begin{pmatrix} \mathbb{T}_1 & \mathbb{T}_{1,2} & \cdots & \mathbb{T}_{1,t} \\ \mathbb{O} & \mathbb{T}_2 & \cdots & \mathbb{T}_{2,t} \\ \vdots & \ddots & \ddots & \vdots \\ \mathbb{O} & \cdots & \mathbb{O} & \mathbb{T}_t \end{pmatrix}.$$

Matrix $\widetilde{\mathbb{A}}$ would have the same structure as, e.g., $\widetilde{\mathbb{P}}_{\mathcal{T}\to\mathcal{T}}$ shown in Eq. (3), where each $\mathbb{T}_i$ and $\mathbb{T}_{i,j}$ are irreducible. Fig. 7 gives an example of the underlying DAG of $\widetilde{\mathbb{A}}$ for $t = 6$, assuming that all of the upper triangular block matrices are non-zero.

Let $\mathbb{M}_i \equiv (\mathbb{1} - \mathbb{T}_i)^{-1}$ and $S(i,j)$ be the set of all possible subsets of $\{i, i+1, \ldots, j\}$ with i and j as the first and the last elements, and is listed in increasing order. For example, $S(1,4) = \{\{1,2,3,4\},\{1,2,4\},\{1,3,4\},\{1,4\}\}$. One can recursively apply Eq. (13) to compute the inverse of

$$\widetilde{\mathbb{D}} = \mathbb{1} - \widetilde{\mathbb{A}} = \begin{pmatrix} \mathbb{1}-\mathbb{T}_1 & -\mathbb{T}_{1,2} & \cdots & -\mathbb{T}_{1,t} \\ \mathbb{O} & \mathbb{1}-\mathbb{T}_2 & \cdots & -\mathbb{T}_{2,t} \\ \vdots & \ddots & \ddots & \vdots \\ \mathbb{O} & \cdots & \mathbb{O} & \mathbb{1}-\mathbb{T}_t \end{pmatrix}. \tag{14}$$

It is straightforward to show that the $(i,j)^{\text{th}}$ block component of $\widetilde{\mathbb{D}}^{-1}$ is given

by

$$\left[\widetilde{\mathbb{D}}^{-1}\right]_{i,j} = \begin{cases} \mathbb{M}_i & i = j, \\ \mathbb{M}_i \cdot \sum_{s \in S(i,j)} \prod_{k=1}^{\|s\|-1} \left(\mathbb{T}_{s_k,s_{k+1}} \cdot \mathbb{M}_{s_{k+1}}\right) & i < j, \\ \mathbb{O} & i > j. \end{cases} \tag{15}$$

The sum in the case of $i < j$ is taken over all members s of $S(i,j)$, where s_k denotes the k^{th} element of s and $\| s \|$ denotes the number of elements. Once the inverses of all block elements are computed and the whole $\widetilde{\mathbb{D}}^{-1}$ is assembled, one can simply perform another change of basis to shuffle all elements back to their original orders.

Eq. (15) may be conveniently read off from the structure of the DAG of $\widetilde{\mathbb{A}}$. To obtain the $(i,j)^{\text{th}}$ block component, one simply traverses the graph from node i to j through all possible routes. Each visit to node k corresponds with $\mathbb{M}_k$. Each passage through an edge from l to m corresponds with $\mathbb{T}_{l,m}$. The final result is the sum over these routes. This method amounts to graph traversal which is a common routine in graph programming.

Our method of finding an inverse not only is simple, but also reveals the fundamental structure of the matrix. Moreover, in some problems, only a small subset of inverse matrix elements are needed. Our method would tremendously reduce the amount of computation because only a few $\mathbb{M}_i$'s may be required. Finally we should point out that directly finding $\mathbb{A}^{-1}$ is not much harder than finding $\mathbb{D}^{-1}$. The additional difficulty arises in keeping track of extra minus signs that crops up depending on whether the number of $\mathbb{T}_{l,m}$'s in an expression is odd or even. This could be done simply by counting the number of nodes visited during the traversal.

B References

[1] F. D. A. Aarão Reis, *Dynamic scaling in thin-film growth with irreversible step-edge attachment*, Phys. Rev. E **81** (2010), 041605.

[2] Réka Albert and Albert-László Barabási, *Statistical mechanics of complex networks*, Rev. Mod. Phys. **74** (2002), 47–97.

[3] Grazyna Antczak and Gert Ehrlich, *Jump processes in surface diffusion*, Surf. Sci. Repo. **62** (2007), 39–61.

[4] ———, *Asymmetric one-dimensional random walks*, J. Chem. Phys. **129** (2008), 124702.

[5] Bengt Aspvall, Michael F. Plass, and Robert E. Tarjan, *A linear-time algorithm for testing the truth of certain quantified boolean formulas*, Inform. Process. Lett. **8** (1979), no. 3, 121–3.

[6] Abraham Berman and Robert J. Plemmons, *Nonnegative matrices in the mathematical sciences*, SIAM, Philadelphia, 1994.

[7] S. Boccaletti, V. Latora, Y. Moreno, M. Chavez, and D.-U. Hwang, *Complex networks: Structure and dynamics*, Phys. Repo. **424** (2006), 175–308.

[8] W. K. Burton, N. Cabrera, and F. C. Frank, *The growth of crystals and the equilibrium structure of their surfaces*, Phil. Trans. R. Soc. (Lond.) A **243** (1951), 299.

[9] N. Cabrera and M. M. Levine, Philos. Mag. **1** (1956), 450.

[10] Fan R. K. Chung, *Spectral graph theory*, CBMS Regional Conference Series in Mathematics, no. 92, American Mathematical Society, 1997.

[11] Thomas H. Cormen, Charles E. Leiserson, Ronald L. Rivest, and Clifford Stein, *Introduction to algorithms*, second ed., pp. 552–7, MIT Press and McGraw-Hill, 2001.

[12] Y. Cui and L. Li, *Evolution of spirals during molecular beam epitaxy of GaN on 6H-SiC(0001)*, Phys. Rev. B **66** (2002), 155330.

[13] S. Das Sarma, C. J. Lanczycki, R. Kotlyar, and S. V. Ghaisas, *Scale invariance and dynamical correlations in growth models of molecular beam epitaxy*, Phys. Rev. E **53** (1996), 359–88.

[14] S. Das Sarma and P. I. Tamborenea, *A new universality class for kinetic growth: One-dimensional molecular-beam epitaxy*, Phys. Rev. Lett. **66** (1991), 325–8.

[15] Mario Einax, Wolfgang Dieterich, and Philipp Maass, *Colloquium: Cluster growth on surfaces: Densities, size distributions, and morphologies*, Rev. Mod. Phys. **85** (2013), 921.

[16] Georg Frobenius, *Über Matrizen aus nicht negativen Elementen*, Sitzungsber. Königl. Preuss. Akad. Wiss. (1912), 456–77.

[17] C. Gerber, D. Anselmetti, J. G. Bednorz, J. Mannhart, and D. G. Schlom, *Screw dislocation in high-t_c films*, Nature **350** (1991), 279–80.

[18] G. R. Grimmett and D. R. Stirzaker, *Probability and random processes*, second ed., Oxford University Press, New York, 1992.

[19] Gregory Grochola, Ian K. Snook, and Salvy P. Russo, *Static substrate deposition: Toward longer time scale deposition simulations*, Phys. Rev. B **84** (2011), 165442.

[20] B. Heying, E. J. Tarsa, C. R. Elsass, P. Fini, S. P. DenBaars, and J. S. Speck, *Dislocation mediated surface morphology of GaN*, J. Appl. Phys. **85** (1999), no. 9, 6470–6.

[21] J. P. Jarvis and D. R. Shier, *Graph-theoretic analysis of finite Markov chains*, Applied Mathematical Modeling: A Multidisciplinary Approach (D. R. Shier and K. T. Wallenius, eds.), CRC Press, 1999, pp. 271–89.

[22] A. B. Kahn, *Topological sorting of large networks*, Communications of the ACM **5** (1962), no. 11, 558–62.

[23] Alain Karma and Mathis Plapp, *Spiral surface growth without desorption*, Phys. Rev. Lett. **81** (1998), no. 20, 4444.

[24] T. R. Linderoth, S. Horch, E. Lægsgaard, I. Stensgaard, and F. Besenbacher, *Surface diffusion of Pt on Pt(110): Arrhenius behavior of long jumps*, Phys. Rev. Lett. **78** (1997), no. 26, 4978–81.

[25] L. Lovász, *Random walks on graphs: A survey*, Combinatorics: Paul Erdos is Eighty (D. Miklos, V. T. Sos, and T. Szonyi, eds.), vol. 2, Bolyai Society Mathematical Studies, 1993, pp. 1–46.

[26] Carl D. Meyer, *Matrix analysis and applied linear algebra*, SIAM, Philadelphia, 2000.

[27] Stephen A. Morin and Song Jin, *Screw dislocation-driven epitaxial solution growth of ZnO nanowires seeded by dislocaions in GaN substrates*, Nano Lett. **10** (2010), 3459–63.

[28] M. E. J. Newman, *Networks: An introduction*, Oxford University Press Inc., New York, 2010.

[29] Sang-Mun Oh, Seong Jin Koh, Kentaro Kyuno, and Gert Ehrlich, *Non-nearest-neighbor jumps in 2D diffusion: Pd on W(110)*, Phys. Rev. Lett. **88** (2002), no. 23, 236102.

[30] K. Oura, V. G. Lifshits, A. A. Saranin, A. V. Zotov, and M. Katayama, *Surface science: An introduction*, ch. 13, Springer-Verlag, Berlin, Germany, 2003.

[31] G. Palasantzas and J. Krim, *Scanning tunneling microscopy study of thick film limit of kinetic roughening*, Phys. Rev. Lett. **73** (1994), 3564–7.

[32] A. Parkhomovsky, A. M. Dabiran, B. Benjaminsson, and P. I. Cohen, *Hexagonal growth spirals on GaN grown by molecular-beam epitaxy: kinetics versus thermodynamics*, Appl. Phys. Lett. **78** (2001), no. 16, 2315–7.

[33] Oskar Perron, *Zur theorie der matrices*, Mathematische Annalen **64** (1907), no. 2, 248–63.

[34] Alex Redinger, Oliver Ricken, Philipp Kuhn, Andreas Rätz, Axel Voigt, Joachim Krug, and Thomas Michely, *Spiral growth and step edge barriers*, Phys. Rev. Lett. **100** (2008), 035506.

[35] Yunsic Shim and Jacques G. Amar, *Semirigorous synchronous sublattice algorithm for parallel kinetic Monte Carlo simulations of thin film growth*, Phys. Rev. B **71** (2005), 125432.

[36] ———, *Reaching extended length scales and time scales in atomistic simulations via spatially parallel temperature-accelerated dynamics*, Phys. Rev. B **76** (2007), 205439.

[37] ———, *Adaptive temperature-accelerated dynamics*, J. Chem. Phys. **134** (2011), 054127.

[38] G. Springholz, A. Y. Ueta, N. Frank, and G. Bauer, *Spiral growth and threading dislocations for molecular beam epitaxy of PbTe on BaF_2 (111) studied by scanning tunneling microscopy*, Appl. Phys. Lett. **69** (1996), no. 19, 2822–4.

[39] Steven H. Strogatz, *Exploring complex networks*, Nature **410** (2001), 268–76.

[40] P. I. Tamborenea and S. Das Sarma, *Surface-diffusion-driven kinetic growth on one-dimensional substrates*, Phys. Rev. E **48** (1993), 2575–94.

[41] Chao Tang, *Diffusion-limited aggregation and the Saffman-Taylor problem*, Phys. Rev. A **31** (1985), 1977–9.

[42] Robert E. Tarjan, *Edge-disjoint spanning trees and depth-first search*, Algorithmica **6** (1976), no. 2, 171–85.

[43] Richard S. Varga, *Matrix iterative analysis*, 2nd ed., Springer-Verlag, 2000.

[44] S. C. Wang, J. D. Wrigley, and Gert Ehrlich, *Atomic jump lengths in surface diffusion: Re, Mo, Ir, and Rh on W(211)*, J. Chem. Phys. **91** (1989), 5087.

[45] D. E. Wolf and J. Villain, *Growth with surface diffusion*, Europhys. Lett. **13** (1990), no. 5, 389–94.

[46] Rong-Fu Xiao, J. Iwan, D. Alexander, and Franz Rosenberger, *Morphological evolution of growing crystals: A Monte Carlo simulation*, Phys. Rev. A **38** (1988), 2447–56.

[47] ———, *Growth morphologies of crystal surfaces*, Phys. Rev. A **43** (1991), no. 6, 2977–92.

[48] ———, *Simulation of surface morphologies in crystal growth from the vapor*, J. Cryst. Growth **109** (1991), 43–9.

[49] Yan-Mei Yu, Bang-Gui Liu, and Axel Voigt, *Phase-field modeling of anomalous spiral step growth on Si(001) surface*, Phys. Rev. B **79** (2009), 235317.

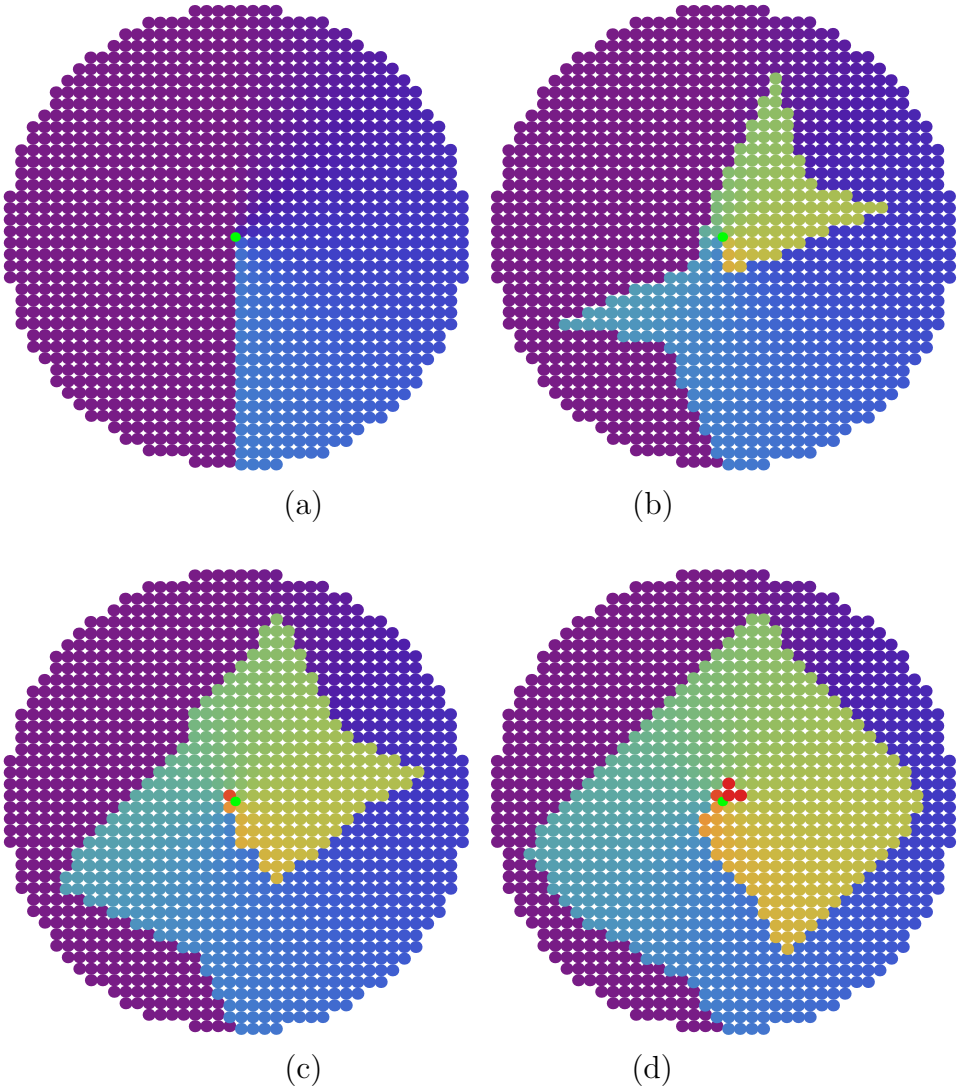

Figure 5: Growth around a screw dislocation starting from (a) initial profile, then after (b) 200 atoms, (c) 400 atoms, and (d) 600 atoms are deposited.

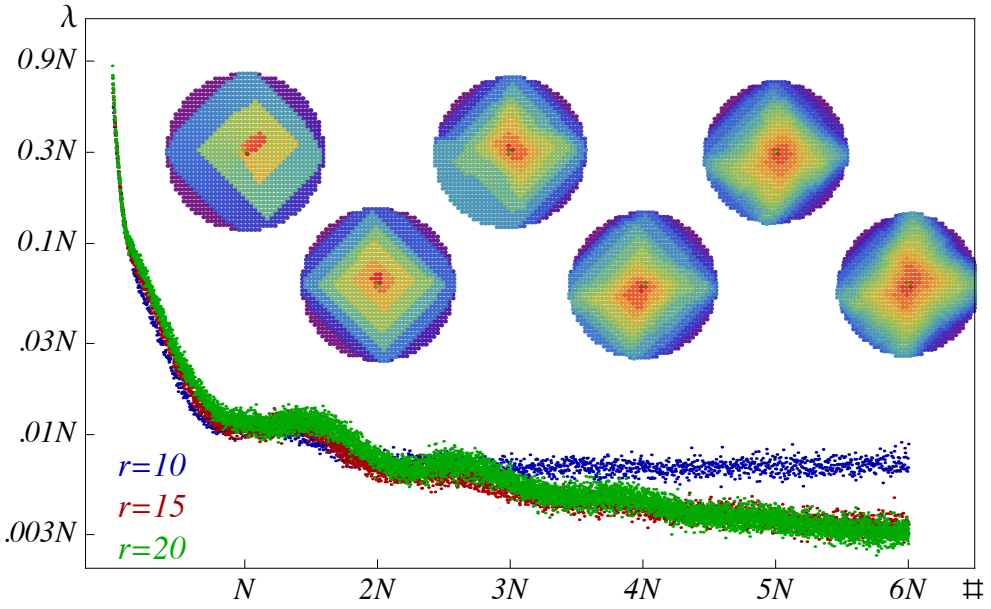

Figure 6: The average mean free path λ simulated by Method I and measured in the units of the respected number of sites N is plot as a function of subsequent drops up to the $6N^{\text{th}}$ atom for circular substrate of radius 10, 15 and 20 as shown in blue (black), red (dark gray) and green (light gray) respectively. The surface profile after every N^{th} deposited atoms simulated by Method II are shown as points of reference.

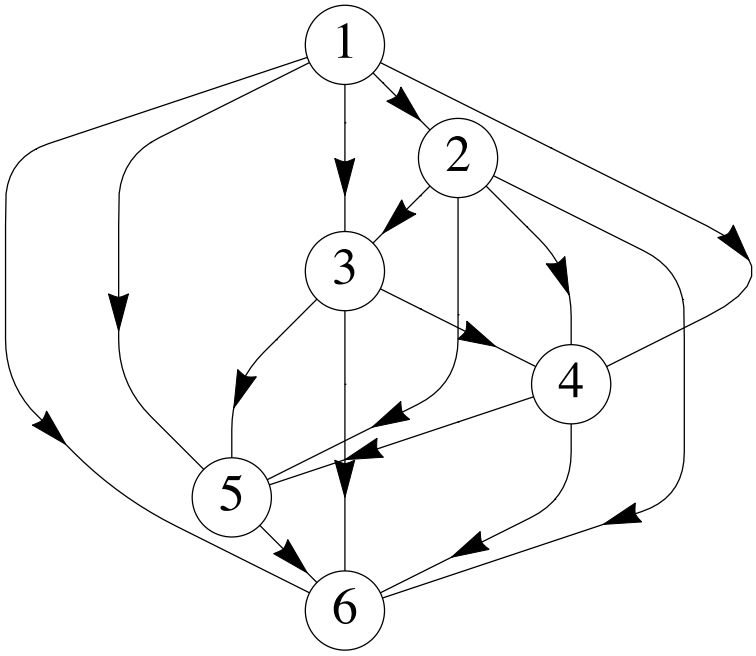

Figure 7: An example of a directed acyclic graph representing a matrix in its canonical form.

ผลผลิตจากงานวิจัย

ผลผลิตจากโครงการวิจัย

1. ผลงานตีพิมพ์ในวารสารวิชาการนานาชาติ

   S. Limkumnerd, *Random walk on lattices: Graph-theoretic approach to simulating long-range diffusion-attachment growth models*, Phys. Rev. E **89** (2014), 032402. Impact Factor 2.400

2. การนำผลงานวิจัยไปใช้ประโยชน์

   <u>เชิงสาธารณะ</u>: งานวิจัยชิ้นนี้เป็นการศึกษาลักษณะทางกายภาพของฟิล์มบางในการปลูกแบบโมเลกุลาร์บีมเอพิแทกซี ซึ่งสามารถนำไปใช้ต่อยอดในด้านอุตสาหกรรมการปลูกฟิล์มบางได้ เนื่องจากการปลูกฟิล์มบางจำเป็นอย่างยิ่งที่จะต้องควบคุมความขรุขระของแต่ละชั้นฟิล์ม โดยงานวิจัยชิ้นนี้เป็นส่วนหนึ่งของการศึกษาในลักษณะเดียวกันภายในศูนย์วิจัยทางฟิสิกส์ของฟิล์มบาง (Research Center in Thin Film Physics) ซึ่งเป็นส่วนหนึ่งของศูนย์ความเป็นเลิศด้านฟิสิกส์ (Thailand Center of Excellence in Physics: ThEP) ทำให้งานวิจัยชิ้นนี้ได้รับความสนใจจากผู้วิจัยภายในศูนย์ซึ่งประกอบด้วยคณาจารย์จาก 5 สถาบันการศึกษาของรัฐ

   <u>เชิงวิชาการ</u>: งานวิจัยชิ้นนี้สามารถนำไปต่อยอดเพื่อใช้ในการคำนวณลักษณะความเป็นไปได้ของผิวฟิล์มในอนาคตจากรูปร่างของพื้นผิวของสับสเตรทตอนเริ่มต้นได้ ซึ่งจะนำไปสู่ความสามารถในการควบคุมลักษณะผิวฟิล์มที่ต้องการในการปลูกได้

3. ผลงานได้นำไปเสนอในการประชุมวิชาการต่าง ๆ ดังนี้

   3.1 “Graph Theoretic Approach to Modelling Epitaxially Grown Thin Films,” นักวิจัยรุ่นใหม่ พบ เมธีวิจัยอาวุโส สกว. ครั้งที่ 10, ณ โรงแรมฮอลิเดย์อินน์ รีสอร์ท รีเจนท์ บีช ชะอำ วันที่ 14-16 ตุลาคม 2553.

   3.2 “Graph Theoretic Approach to Modelling Epitaxially Grown Thin Films,” Siam Physics Congress 2011, Ambassador Hotel, Pattaya, March 24-26 2011.

ภาคผนวก

บทความสำหรับการเผยแพร่

ชื่อเรื่อง (อังกฤษ) Random walk on lattices: Graph-theoretic approach to simulating long-range diffusion-attachment growth models

ชื่อเรื่อง (ไทย) การเดินแบบสุ่มบนผลึก: กระบวนการจำลองการเติบโตแบบแพร่เกาะยึดระยะไกลด้วยทฤษฎีกราฟ

งานวิจัยชิ้นนี้เป็นการพัฒนาการจำลองการปลูกฟิล์มบางแบบโมเลกุลาร์บีมเอพิแทกซี (การปลูกฟิล์มบางโดยการปูอะตอมเป็นระนาบ) ให้สามารถจำลองลักษณะของพื้นผิวที่เกิดจากการที่อะตอมสามารถเคลื่อนที่เป็นระยะทางไกลได้ ก่อนหน้านี้มีแบบจำลองการปลูกฟิล์มอยู่แล้วเป็นจำนวนมาก แต่แบบจำลองส่วนใหญ่จำกัดระยะการเคลื่อนที่ของอะตอมให้ไปได้เฉพาะตำแหน่งที่ใกล้กับบริเวณที่อะตอมตกเท่านั้น การจะทำให้อะตอมเคลื่อนที่ได้ไกลกว่านั้นจำเป็นที่จะต้องใช้การจำลองซ้ำเดิมครั้งแล้วครั้งเล่า จะเห็นได้ว่าอัลกอริทึมแบบนี้เป็นการสิ้นเปลืองทรัพยากรคอมพิวเตอร์สำหรับการคำนวณเป็นอย่างมาก และผลสัมฤทธิ์ก็ยังไม่ได้รูปร่างของผิวฟิล์มที่เป็นตัวแทนเชิงสถิติที่ดีนัก ในงานวิจัยชิ้นนี้ ผู้วิจัยหลักได้ใช้ทฤษฎีกราฟผนวกกับทฤษฎีการเคลื่อนที่แบบสุ่มเพื่อใช้ในการจำลองลักษณะการเคลื่อนที่ของอะตอมภายใต้กฎการเคลื่อนที่ที่กำหนด ผลที่ได้คือ เราสามารถทราบตำแหน่งที่อะตอมอยากจะเคลื่อนที่ไปถึงด้วยค่าความน่าจะเป็นชัดเจนทางทฤษฎี นอกจากนี้เรายังสามารถคำนวณปริมาณต่าง ๆ ทางสถิติ เช่น จำนวนก้าวเฉลี่ยของอะตอมระหว่างการปลูก ซึ่งเป็นค่าที่ไม่สามารถคำนวณได้มาก่อนด้วยการจำลองแบบเก่า บทความชิ้นนี้เป็นจุดเริ่มต้นในการจำลองหาลักษณะของผิวฟิล์มที่ปลูกในห้องปฏิบัติการ อันจะนำไปสู่การหาสภาวะที่เหมาะสมในการปลูกฟิล์มที่จะส่งผลให้ได้ผิวฟิล์มที่ตามต้องการ ซึ่งจะเป็นประโยชน์อย่างมากทั้งในเชิงวิจัยและเชิงอุตสาหกรรม

Random walk on lattices: Graph-theoretic approach to simulating long-range diffusion-attachment growth models

Surachate Limkumnerd*

Department of Physics, Faculty of Science, Chulalongkorn University, Phayathai Road, Patumwan, Bangkok 10330, Thailand and Research Center in Thin Film Physics, Thailand Center of Excellence in Physics, CHE, 328 Si Ayutthaya Road, Bangkok 10400, Thailand

(Received 4 September 2013; revised manuscript received 4 February 2014; published 11 March 2014)

Interest in thin-film fabrication for industrial applications have driven both theoretical and computational aspects of modeling its growth. One of the earliest attempts toward understanding the morphological structure of a film's surface is through a class of solid-on-solid limited-mobility growth models such as the Family, Wolf-Villain, or Das Sarma–Tamborenea models, which have produced fascinating surface roughening behaviors. These models, however, restrict the motion of an incidence atom to be within the neighborhood of its landing site, which renders them inept for simulating long-distance surface diffusion such as that observed in thin-film growth using a molecular-beam epitaxy technique. Naive extension of these models by repeatedly applying the local diffusion rules for each hop to simulate large diffusion length can be computationally very costly when certain statistical aspects are demanded. We present a graph-theoretic approach to simulating a long-range diffusion-attachment growth model. Using the Markovian assumption and given a local diffusion bias, we derive the transition probabilities for a random walker to traverse from one lattice site to the others after a large, possibly infinite, number of steps. Only computation with linear-time complexity is required for the surface morphology calculation without other probabilistic measures. The formalism is applied, as illustrations, to simulate surface growth on a two-dimensional flat substrate and around a screw dislocation under the modified Wolf-Villain diffusion rule. A rectangular spiral ridge is observed in the latter case with a smooth front feature similar to that obtained from simulations using the well-known multiple registration technique. An algorithm for computing the inverse of a class of substochastic matrices is derived as a corollary.

DOI: 10.1103/PhysRevE.89.032402 PACS number(s): 81.15.Aa, 68.35.Fx, 68.55.A−

I. INTRODUCTION

Limited mobility solid-on-solid diffusion models as means to study surface growth continue to attract much interest even after decades of investigations both computationally and analytically. In the Wolf-Villain (WV) model [1], an adatom moves in the direction that *maximizes* its coordination number in the next discrete time step, while in the Das Sarma–Tamborenea (DT) model [2], it moves to *increase* the number, provided that the current one is not sufficiently high. In both models, and others like them, an adatom moves one lateral step before coming to a halt. Despite their simplicity, they are found to yield consistent simulation results with more realistic finite-temperature model using Arrhenius hopping rate [3] and low-temperature molecular-beam epitaxy (MBE) experiments [4]. These models, however, are inadequate as tools to investigate surface evolution in cases where each adatom undergoes a large number of hops before it is embedded as part of the surface. The simplest extension of these models to mimic a large diffusion length by repeated applications of one-step motion cannot avoid prescribing an *ad hoc* maximum cutoff distance, and often is too computationally intensive for problems which require large-scale and/or long-time simulations. Furthermore, this basic approach does not give any statistics of the growth in any straightforward way. A more systematic approach is needed. The aim of this paper is to present a graph-based method to model long-ranged solid-on-solid diffusion-attachment surface growth where, one at a time, an adatom is deposited onto a surface where each hop is determined by the local environment and is independent of the previous ones. Our method can, in principle, provide statistics, such as the average mean free path of growth particles, and give the most probable surface pattern under any given lattice structure and local diffusion rule.

Graph theory has been at the core of mathematics and computer science and has recently fueled considerable interests in understanding the behaviors of complex networks [5]. One of the theory's vast applications is in the development of random walks on graphs [6] where a random walker traverses from one vertex to subsequent ones along (possibly weighted) edges connecting them. To use this idea to model surface growth on a lattice due to long-range adatom diffusion, we construct a graph whose vertex i represents a lattice position and stores in it relevant lattice-dependent properties (such as atomic height at that point). An edge connecting two neighboring vertices i and k signifies a nonzero probability P_{ik} of an adatom; if present at i, it would hop to k. This hop thus decreases the height value stored in i and increases that stored in k by one unit. The weight of each edge can be obtained, as is the case here, from a chosen diffusion model such as WV or DT or from a more realistic calculation using density functional theory. Through this graph, we establish the most likely final position of a deposited atom whose trip begins at i, and the average number of hops it takes to get there. By repeating this process, the surface is evolved.

To test our method, we choose to apply it to simulating the spiral surface growth around a screw dislocation commonly observed in MBE grown films with lattice mismatch at the film-substrate interface, such as that of GaN-based devices [7] or certain semiconductor materials [8], and is known to provide a mechanism for driving the growth of a class of nanowires [9].

*surachate.l@chula.ac.th

Unlike the spiral growth in the limit of fast desorption, where the ridge motion can be determined locally and is well described by the Burton-Cabrera-Frank (BCF) model [10], the minimal desorption limit where the particle's diffusion length is comparable to the system size still presents a modeling challenge. Theoretical and computational investigations of spiral growth in this regime are typically carried out in a continuum limit using a phase-field method [11]. This method, although it provides an analytical handle to the problem, suffers from the shortcomings of a continuum formulation, e.g., when accounting for system's anisotropy. The kinetic Monte Carlo (kMC) method has also been chosen to explore the spiral growth [12]. In order to suppress microscopic noise, either the use of multiple-registration [13] or atomic evaporation [12] schemes must be implemented. The latter, though more realistic, is less practical at the extremely low supersaturation limit being considered.

The paper is organized as follows. The mathematical structures will be discussed in Sec. II where surface sites are classified (Sec. II A) and the limiting lattice transitions are calculated (Sec. II B). Implementation and graph algorithms will be mentioned in Sec. II C. The formalism is applied using the modified Wolf-Villain model on a two-dimensional solid-on-solid surface growth on an originally flat substrate (Sec. III A) and around a single screw dislocation (Sec. III B). Results will be discussed in Sec. IV, followed by concluding remarks in Sec. V.

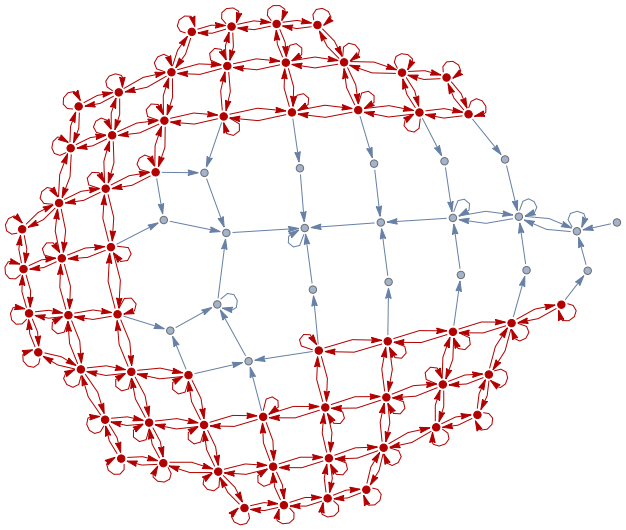

FIG. 1. (Color online) A graph representation of a transition matrix whose vertices symbolize states of the system in terms of an adatom's position. Each arrow depicts an edge linking two positions whose transition probability from one to the other is nonzero. The probability is derived from WV diffusion rule on a circularly shaped substrate with a screw dislocation. One can see the trace of the underlying simple cubic lattice structure from the graph. Vertices and edges in red (dark gray) show a part of the graph which is strongly connected. These vertices form a class.

II. MATHEMATICAL CONSTRUCT

The mathematical question underlying our modeling of particle diffusion with possibly infinite diffusion length amounts to finding the probability that a random walker beginning its journey at position i on a lattice would reach the far-away point j by traveling along the edges connecting them. Edges linking, say, vertex i to its neighbors are not necessarily of equal weights. Biased or asymmetric walks are accounted for by having directed weighted edges. This type of walk is required for modeling diffusion in the presence of fields such as in electromigration [14] or when adatoms sensitively react to local atomic configurations. The Markovian assumption that each step the walker takes is independent of the previous one was proven to be quite accurate [15]. If only nearest-neighbor hopping is allowed, only edges linking nearest neighbors are present and the graph structure matches the structure of the lattice surface. In principle one can incorporate long atomic jumps by including edges linking remote sites with a suitable weight factor. This type of jump has been observed experimentally with fairly significant jump rates [16]. For simplicity, we shall only limit ourselves to one random walker. This allows us to easily define a system's state at a given time by the lattice position of the walker. A more complicated scheme is required to define a state should one choose to model, e.g., clustered or collective diffusion [17].

In this section, we shall outline the relevant portions of discrete time Markov chain needed for the modeling and state our graph algorithm for computing the infinite-hop transition matrix. For an illustrative purpose, we shall phrase the problem in the language of crystal growth where an adatom wanders from point i to point j according to a given set of diffusion rules by hopping between atomic positions (vertices) linking i and j. Let a lattice configuration, some lattice-dependent property which influences the probability of the adatom such as atomic heights, be described by $\vec{H} \equiv \{H_i\}$. Define a one-step transition matrix $\mathbb{P}(\vec{H})$ whose element $P_{ik}(\vec{H})$ gives a transition probability for an atom at i to go to one of the connecting sites k which usually is a nearest-neighboring lattice site. A nonzero element P_{ik} is thus equivalent to having a directed edge with a corresponding probabilistic weight connecting vertex i to vertex k of a graph as shown, for example, in Fig. 1. We also account for in-place hopping through the matrix element P_{ii} (represented graphically by a vertex with self-loop). Since the adatom must go somewhere $\sum_k P_{ik} = 1$, which makes $\mathbb{P}$ a stochastic matrix. Knowing $\mathbb{P}$, one can easily find the transition probability from i to j if the atom takes *exactly* n hops using

$$P_{ij}^{(n)} = \sum_k P_{ik} P_{kj}^{(n-1)} = \sum_{k_1,k_2,\ldots,k_{n-1}} P_{ik_1} \cdots P_{k_{n-1}j}, \quad (1)$$

or, simply, $\mathbb{P}^{(n)} = \mathbb{P}^n$ in matrix notation. Since we are interested in the long diffusion limit, we shall investigate in particular the case where $n \to \infty$.

A. Lattice site classification

Given the state of height configuration $\vec{H}$, one can classify lattice position j (or the system's state) according to the limiting behavior of $\mathbb{P}^\infty$ into *transient class* (denoted by $\mathcal{T}$) or *recurrent class* (denoted by $\mathcal{R}$). In the case of a finite number of a system's states [18] (which is particularly relevant for modeling Markov processes on a computer), j is transient if

$P_{ij}^{\infty} = 0$ and recurrent otherwise.[1] Loosely speaking, if one lets an adatom wander for a very long time, it will end up at one of the recurrent sites. It is easy to see that there must be at least one such site, otherwise $P_{ij}^{\infty} = 0$ for all j with edge(s) directed from i. This would lead to $\sum_j P_{ij}^{\infty} = 0$ and we would reach a contradiction because the adatom starting from i must go somewhere. The real merit of this classification is that it can be done through permuting rows and columns of $\mathbb{P}$ which amounts to relabeling of lattice positions, and prior to the actual computation of $\mathbb{P}^{\infty}$ itself.

If $\mathbb{P}$ is reducible, i.e., if there exists at least one transient site, then by definition one can find a nonunique permutation matrix $\mathbb{Q}_1$ that transforms $\mathbb{P}$ into a block triangular form such that $\mathbb{Q}_1^{\top} \cdot \mathbb{P} \cdot \mathbb{Q}_1 = \left(\begin{smallmatrix} \mathbb{X} & \mathbb{Y} \\ \mathbb{O} & \mathbb{Z} \end{smallmatrix}\right)$, where $\mathbb{X}$ and $\mathbb{Z}$ are square matrices, and $\mathbb{O}$ is a matrix with all elements being zero. If $\mathbb{X}$ and $\mathbb{Z}$ are reducible still, then we can apply another symmetric permutation to them. If during the process there exist rows with nonzero entries only in diagonal blocks, these rows can be permuted to the bottom of the modified transition matrix. Finally, we shall arrive at the upper-triangular block form or the *canonical form for reducible matrices* [19] of a system via permutation matrix $\mathbb{Q}$ formed from the products of previous permutation matrices,

$$\widetilde{\mathbb{P}} = \mathbb{Q}^{\top} \cdot \mathbb{P} \cdot \mathbb{Q} = \begin{pmatrix} \widetilde{\mathbb{P}}_{\mathcal{T}\to\mathcal{T}} & \widetilde{\mathbb{P}}_{\mathcal{T}\to\mathcal{R}} \\ \mathbb{O} & \widetilde{\mathbb{P}}_{\mathcal{R}\to\mathcal{R}} \end{pmatrix}, \tag{2}$$

where

$$\widetilde{\mathbb{P}}_{\mathcal{T}\to\mathcal{T}} = \begin{pmatrix} \mathbb{T}_1 & \mathbb{T}_{1,2} & \cdots & \mathbb{T}_{1,t} \\ \mathbb{O} & \mathbb{T}_2 & \cdots & \mathbb{T}_{2,t} \\ \vdots & \ddots & \ddots & \vdots \\ \mathbb{O} & \cdots & \mathbb{O} & \mathbb{T}_t \end{pmatrix},$$

$$\widetilde{\mathbb{P}}_{\mathcal{T}\to\mathcal{R}} = \begin{pmatrix} \mathbb{S}_{1,1} & \cdots & \mathbb{S}_{1,r} \\ \vdots & \ddots & \vdots \\ \mathbb{S}_{t,1} & \cdots & \mathbb{S}_{t,r} \end{pmatrix}, \tag{3}$$

$$\widetilde{\mathbb{P}}_{\mathcal{R}\to\mathcal{R}} = \begin{pmatrix} \mathbb{R}_1 & & \mathbb{O} \\ & \ddots & \\ \mathbb{O} & & \mathbb{R}_r \end{pmatrix}.$$

Each diagonal block matrix $\mathbb{T}_1, \ldots, \mathbb{T}_t$ is either irreducible or $\mathbb{O}$ and $\mathbb{R}_1, \ldots, \mathbb{R}_r$ are irreducible and stochastic. In the language of graphs, the graph representation of matrix $\mathbb{A}$ is irreducible if there is a sequence of directed edges linking every pair of vertices together, i.e., the graph is *strongly connected*. As an example, the vertices and edges highlighted in red (dark gray) in Fig. 1 make up a subgraph which is strongly connected. Thus their transition matrix representation is irreducible.

[1] In particular these recurrent states are non-null. For $j \in \mathcal{R}$, it is non-null if $\mu_j \equiv \sum_{n=0}^{\infty} n F_{jj}^n$ is finite. Here F_{ij}^n is the first passage probability which denotes the likelihood that a walker starting at i will end up at j for the first time after exactly n hops. Thus μ_j gives mean recurrence time of state j or the expected value of the time of the first visit to j from j.

Through the application of $\mathbb{Q}$, the newly ordered, one-step transition matrix $\widetilde{\mathbb{P}}$ shows the separations of lattice sites into t transient classes $\mathcal{T}_1, \ldots, \mathcal{T}_t$, and r recurrent classes $\mathcal{R}_1, \ldots, \mathcal{R}_r$. The form also effectively suggests from which transient classes is a site in a recurrent class *accessible*.[2] It is therefore of paramount importance to devise an algorithm to construct $\mathbb{Q}$. We shall postpone this discussion to Sec. II C.

B. Limiting lattice transitions

To arrive at the limiting transition probability matrix $\mathbb{P}^{\infty}$, one is interested in examining the possibility of transitions between elements in $\mathcal{T}$ and/or $\mathcal{R}$. We shall state without proofs these results [19], some of which are most evident from the structure of $\widetilde{\mathbb{P}}$ in Eqs. (2) and (3). The following transitions from i to j lead to vanishing probability, $P_{ij}^{\infty} = 0$: (a) $i, j \in \mathcal{T}$, (b) $i \in \mathcal{R}_1$ but $j \in \mathcal{R}_2$, and (c) $i \in \mathcal{R}$ and $j \in \mathcal{T}$. In other words, after a large number of hops, if a random walker beginning its trip from any of the transient classes, it will eventually go to a recurrent class. If, however, it already starts its journey in one of the recurrent classes, it will stay there forever. The remarkable theorem due to Oskar Perron and Georg Froebenius [20] enables us to compute the limiting probability distribution of the latter case when it exists and otherwise provides the fraction of time the walker spends on each site in the class.

When a random walker starts its trip within a recurrent class, say, $\mathcal{R}_f$ with m members, whose transition matrix is given by $\mathbb{R}_f$, the fact that the infinite-hop limit of the transition matrix $\mathbb{R}_f^{\infty} \equiv \lim_{n\to\infty} \mathbb{R}_f^n$ exists depends on the periodicity of $\mathbb{R}_f$. Since $\mathbb{R}_f$ is irreducible, it is *aperiodic* if there is only one eigenvalue with modulus 1 and the limit exists, otherwise it is *periodic* and the limit does not exist. A good example of a periodic matrix is $\left(\begin{smallmatrix} 0 & 1 \\ 1 & 0 \end{smallmatrix}\right)$, where each self-multiplication gives the result which fluctuates between itself and the identity matrix. Physically speaking, if a walker enters this class, its position at later times will oscillate between one of the two sites indefinitely. The period of this chain is therefore 2. More generally, the period coincides with the number of eigenvalues of modulus 1.[3] Once in a class, the probability distribution of the walker's positions is not constant in time but continually progresses from subclass to subclass and eventually returns to the original distribution after going through all p subclasses. In practice classifying a recurrent class by its periodicity is simple; a non-negative irreducible matrix is aperiodic if there is at least one positive element along the diagonal [19].

[2] Mathematically speaking, site j is said to be accessible from i ($i \to j$) if there is a nonzero probability that, starting from i, the adatom will reach j at some future hop ($P_{ij}^{(n)} > 0$ for some $n \geqslant 0$). Sites i and j communicate with each other ($i \leftrightarrow j$) if and only if $i \to j$ and $j \to i$, which can happen only when both i and j belong to the same class.

[3] Alternatively one can find the period p from the characteristic equation of $\mathbb{R}_f$ without directly computing its eigenvalues. See Ref. [19] for proof.

When the limit exists,

$$\mathbb{R}_f^\infty = \mathbf{e}_f \boldsymbol{\pi}_f^\top = \begin{pmatrix} \pi_{f_1} & \pi_{f_2} & \cdots & \pi_{f_m} \\ \pi_{f_1} & \pi_{f_2} & \cdots & \pi_{f_m} \\ \vdots & \vdots & & \vdots \\ \pi_{f_1} & \pi_{f_2} & \cdots & \pi_{f_m} \end{pmatrix}, \tag{4}$$

where $\mathbf{e}_f$ is a vector whose elements are all 1, and $\boldsymbol{\pi}_f$ is a unique Perron vector satisfying $\mathbb{R}_f^\top \cdot \boldsymbol{\pi}_f = \boldsymbol{\pi}_f$, with all positive elements and properly normalized so $\|\boldsymbol{\pi}_f\|_1 = 1$. This vector represents the distribution of probabilities that the walker will be at a particular site eventually. On the other hand, when $\mathbb{R}_f$ is periodic, $\mathbf{e}_f \boldsymbol{\pi}_f^\top$ in (4) is the solution to the Cesàro average, i.e.,

$$\mathbb{C}_f \equiv \lim_{n\to\infty} \frac{\mathbb{1} + \mathbb{R}_f + \mathbb{R}_f^2 + \cdots + \mathbb{R}_f^n}{n} = \mathbf{e}_f \boldsymbol{\pi}_f^\top. \tag{5}$$

Matrix element $[\mathbb{C}_f]_{ij}$ represents the portion of time that the walker hops onto j irrespectively of its starting position i. Henceforth, for the sake of theoretical discussion, whenever we examine infinite-hop probability within a recurrent class, we shall adopt the Cesàro average interpretation in place of $\mathbb{R}_f^\infty$ when the latter does not exist.

The remaining question is to determine how probable it is for a walker to end up in one of the above recurrent classes if it starts from a transient class. Suppose the hop starts from a site in $\mathcal{T}_s$, the walker might have to visit subsequent intermediate transient classes $\mathcal{T}_m$'s, for all m connecting s to recurrent class $\mathcal{R}_f$. The total probability will ultimately involve how long the walker spends in each class as it traverses. Let matrix element $[\mathbb{M}_s]_{ij}$ denote the expected total number of hops onto site $j \in \mathcal{T}_s$ given that the first hop starts at $i \in \mathcal{T}_s$ and $\mathbb{T}_s$ be the transition probability matrix among members in $\mathcal{T}_s$. Since the walker will either hop onto j with probability $[\mathbb{T}_s^n]_{ij}$, in which case the hop value is 1, or it will not, which brings the hop value to 0. This means $[\mathbb{T}_s^n]_{ij}$ also represents the expected number of hop the walker will step onto j on the n^{th} step. Thus the total number of times the walker steps onto j on average is calculated from the total contributions from all steps,

$$\mathbb{M}_s = \sum_{n=0}^{\infty} \mathbb{T}_s = (\mathbb{1} - \mathbb{T}_s)^{-1}. \tag{6}$$

The non-negativity and irreducibility of $\mathbb{T}_s$ and the fact that all of its eigenvalues have modulus strictly less than 1 ensure that the above Neumann series exists and is positive definite [19]. Matrix $\mathbb{1} - \mathbb{T}_s$ is an example of what is called the *M matrix* and often emerges in relation to systems involving linear or nonlinear equations in many areas, including solving finite difference methods, problems in operations research, and Markov processes [21].

Consider a transient class $\mathcal{T}_{s+1}$ which can be reached only from $\mathcal{T}_s$. The probability that a walker starting at site $i \in \mathcal{T}_s$ will wander to $j \in \mathcal{T}_{s+1}$ after an infinite number of hops must equal the expected period that the walker is going to spend on some site $k \in \mathcal{T}_s$ times the probability that it will exit $\mathcal{T}_s$ through k into $\mathcal{T}_{s+1}$, summing over all transitory sites k's,

$$\sum_{k\in\mathcal{T}_s} [\mathbb{M}_s]_{ik} [\mathbb{T}_{s,s+1}]_{kj} = [\mathbb{M}_s \cdot \mathbb{T}_{s,s+1}]_{ij}. \tag{7}$$

It is easy to extend the result in (7) to the case where there are other intermediate transient classes and/or more than one route for the walker to take until it reaches some chosen transient class $\mathcal{T}_x$. Let $\mathbf{p} = \{p_1, \ldots, p_m\}$ be a path that connects transient class $\mathcal{T}_s$ to $\mathcal{T}_x$ via m intermediate classes $\mathcal{T}_{p_1}, \ldots, \mathcal{T}_{p_m}$. The exiting probability matrix is given by summing over the contributions from all such paths according to

$$\mathbb{P}_{s,x}^{\text{exit}} = \sum_{\mathbf{p}} \mathbb{M}_s \cdot \mathbb{T}_{s,p_1} \cdot \mathbb{M}_{p_1} \cdot \mathbb{T}_{p_1,p_2} \cdots \mathbb{M}_{p_m} \cdot \mathbb{T}_{p_m,x}. \tag{8}$$

Moreover, the probability that the walker in $\mathcal{T}_x$ will transit to $\mathcal{R}_f$ is simply $\mathbb{M}_x \cdot \mathbb{S}_{x,f}$. Combining this result with (8), we finally arrive at the expression for the probability that a walker starting from a site in $\mathcal{T}_s$ will be entrapped in $\mathcal{R}_f$ after a large number of hops,

$$\mathbb{S}_{s,f}^\infty = \sum_x \mathbb{P}_{s,x}^{\text{exit}} \cdot \mathbb{M}_x \cdot \mathbb{S}_{x,f} \cdot \mathbb{R}_f^\infty. \tag{9}$$

The sum $\sum_x$ is taken over all possible $\mathcal{T}_x$'s from which $\mathcal{R}_f$ can be accessible.

The result of this analysis can be summarized by the following matrix:

$$\widetilde{\mathbb{P}}^\infty = \begin{pmatrix} \mathbb{0} & \cdots & \mathbb{0} & \mathbb{S}_{1,1}^\infty & \cdots & \mathbb{S}_{1,r}^\infty \\ \vdots & \ddots & \vdots & \vdots & \ddots & \vdots \\ \mathbb{0} & \cdots & \mathbb{0} & \mathbb{S}_{t,1}^\infty & \cdots & \mathbb{S}_{t,r}^\infty \\ \mathbb{0} & \cdots & \mathbb{0} & \mathbb{R}_1^\infty & & \mathbb{0} \\ \vdots & \ddots & \vdots & & \ddots & \\ \mathbb{0} & \cdots & \mathbb{0} & \mathbb{0} & & \mathbb{R}_r^\infty \end{pmatrix}, \tag{10}$$

together with $\mathbb{S}_{s,f}^\infty$ as defined in (9) and $\mathbb{R}_f^\infty$ as in (4) with the appropriate limit interpretation. Given initial state vector $\mathbf{v}_i$, after a large number of hops, the system's probability distribution is therefore

$$\mathbf{v}_f = \mathbf{v}_i \cdot \widetilde{\mathbb{P}}^\infty. \tag{11}$$

C. Graph algorithms

The analysis so far has made full use of the canonical form for reducible matrices. The question thus arises: Is there a way to systematically find a permutation which would cast a reducible matrix into its canonical form? Fortunately, in graph theory there exists a set of algorithms which does exactly this. Initially, one can find a permutation which could swap indices in such a way that strongly connected components (or lattice sites in this case) are grouped together into appropriate classes. Algorithms such as Tarjan's and Gabow's exist to do this with linear-time complexity [22]. At this point, the relationship between classes can be represented by a nonunique *directed acyclic graph* (DAG).

Let $G = (V, E)$ be a DAG with a set of vertices $V = \{1, 2, \ldots, t + r\}$ and a set of edges E. Vertex i represents a transition matrix of type (a) $\mathbb{T}_i$ for all i whose outdegree is positive $[\deg^+(i) > 0]$ or (b) $\mathbb{R}_i$ if i is a *sink* $[\deg^+(i) = 0]$. The underlying graphs of these matrices are, by construction, strongly connected, which make them irreducible. Edge (i, j) connecting vertex i to j represents transition matrix of type

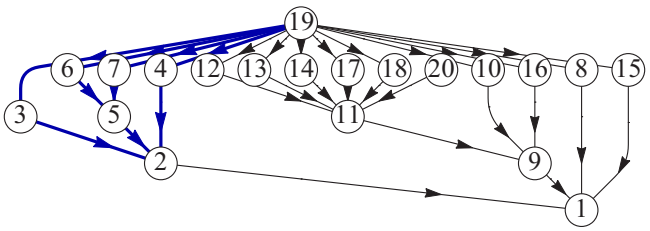

FIG. 2. (Color online) The directed acyclic graph (DAG) of the graph shown in Fig. 1. Each vertex represents a class of strongly connected components, and each edge connects two classes with nonvanishing transition probability from one to the other. Vertex 19, for example, represents the subgraph in Fig. 1 that is highlighted in red (dark gray).

(a) $\mathbb{T}_{i,j}$ from $\mathcal{T}_i$ to $\mathcal{T}_j$ if $\deg^+(j) > 0$ or (b) $\mathbb{S}_{i,j}$ from $\mathcal{T}_i$ to $\mathcal{R}_j$ if j is a sink. An example of such a graph is shown in Fig. 2. Vertices in a DAG have a natural ordering which could best be visualized by a layered tree, pointing one way from vertices of transient classes to those of recurrent classes. A *topological sorting* [23] can be performed in linear time $[\mathcal{O}(|V| + |E|)]$ to yield a permutation of classes from transient to recurrent. By composing the two permutations together, one obtains a permutation which takes a reducible matrix to its canonical form. In practice, it is not important to topologically sort DAG to obtain the full canonical form to efficiently compute elements of $\widetilde{\mathbb{P}}^{\infty}$. The ordering of $\mathbb{M}_a \cdot \mathbb{T}_{a,b}$ terms in Eq. (7) only requires that they appear in the same sequence as the underlying DAG. Topological sorting simply relabels the class numbers in order of appearance, which yields no new information and thus is unnecessary.

In cases where a prescribed diffusion rule prohibits self-hopping ($P_{ii} \neq 0, \forall i$), the limiting probability transition may not exist for some recurrent class $\mathcal{R}_i$. If preferred, one can determine the period of $\mathcal{R}_i$ directly from its underlying subgraph G^i. From a graph-theoretic perspective, G^i is periodic with period p if and only if it can be partitioned into p smaller graphs $G^i_1, \ldots, G^i_p$ such that (a) if vertex m is in G^i_k and an edge (m,n) connects m to n then it is implied that n is in $G^i_{(k+1) \bmod p}$ and (b) p is the largest possible integer with this property. This makes sure that each transition takes the walker to a new class before it returns to the original class after p successive transitions. An aperiodic recurrent class is one where such partition is not possible. The proof of the above theorem and the graph algorithm for finding the period of these "cyclically moving classes" are given in Ref. [24].

To employ G in the limiting probability calculation, we start by assigning appropriate matrices to all vertices and edges. Let $S = \{j \,|\, \deg^+(j) = 0\}$ be the set of all sinks of G. We then assign matrix $\mathbb{M}_i$ to each vertex $i \notin S$, or $\mathbb{R}^{\infty}_i$ for $i \in S$. Each edge (i,j) is prescribed by transition matrix $\mathbb{T}_{i,j}$ for $j \notin S$ and $\mathbb{S}_{i,j}$ for $j \in S$. To compute the limiting probability that a walker would reach a site in one of the recurrent classes in S, we begin by giving the walker his initial probability distribution vector $\mathbf{v}_0$ at the starting class. This vector contains only one nonzero component of value 1 at the position corresponding to the dropped site. Then we scan the graph from the starting vertex (which may or may not be the source) to the sinks. As we traverse the graph to vertex s, we would have accrued all the probability contributions along that path prior to reaching s. The probability distribution $\mathbf{v}_s$ stored at each vertex as it is visited would be

$$\mathbf{v}_s = \begin{cases} \sum_r \mathbf{v}_r \cdot \mathbb{M}_r \cdot \mathbb{T}_{r,s} & \text{if} \quad s \notin S, \\ \left(\sum_r \mathbf{v}_r \cdot \mathbb{M}_r \cdot \mathbb{S}_{r,s}\right) \cdot \mathbb{R}^{\infty}_s & \text{if} \quad s \in S. \end{cases} \tag{12}$$

The above summation $\sum_r$ is taken over all incoming vertices r that point toward s. In a special case where the graph is made up of just one vertex, the final distribution is simply the Perron vector $\boldsymbol{\pi}_s$. It should be emphasized that direct computations of all the $\mathbb{M}_s$ are not necessary. One only needs to calculate $\mathbf{x} \equiv \mathbf{v}_r \cdot \mathbb{M}_r$, which is equivalent to solving the system of linear equations of the form $(\mathbb{1} - \mathbb{T}_r^{\top}) \cdot \mathbf{x} = \mathbf{v}_r$. There exist many iterative schemes to determine $\mathbf{x}$ such as the Jacobi method and the successive over-relaxation (SOR) method [21,25], or one could solve them using the equivalent constrained minimization method. As an illustration, according to the highlighted subgraph of G as shown in Fig. 2 (thick arrows), vertex 2 would receive probability vector $\mathbf{v}_2$ whose value equals

$$\begin{aligned} \mathbf{v}_2 = \mathbf{v}_{19} \cdot \mathbb{M}_{19} \cdot [&\mathbb{T}_{19,3} \cdot \mathbb{M}_3 \cdot \mathbb{T}_{3,2} + \mathbb{T}_{19,4} \cdot \mathbb{M}_4 \cdot \mathbb{T}_{4,2} \\ &+ (\mathbb{T}_{19,6} \cdot \mathbb{M}_6 \cdot \mathbb{T}_{6,5} + \mathbb{T}_{19,7} \cdot \mathbb{M}_7 \cdot \mathbb{T}_{7,5}) \cdot \mathbb{M}_5 \cdot \mathbb{T}_{5,2}]. \end{aligned}$$

Vector $\mathbf{v}_2$ can be interpreted as the probability that a walker would reach each site in transient class $\mathcal{T}_2$ given its initial probability distribution of $\mathbf{v}_{19}$ in class $\mathcal{T}_{19}$. By the time sink 1 is reached, the limiting probability distribution vector $\mathbf{v}_1$ can readily be obtained from the $\mathbf{v}_r$'s of its immediate predecessors as follows:

$$\begin{aligned} \mathbf{v}_1 = [&\mathbf{v}_2 \cdot \mathbb{M}_2 \cdot \mathbb{S}_{2,1} + \mathbf{v}_8 \cdot \mathbb{M}_8 \cdot \mathbb{S}_{8,1} \\ &+ \mathbf{v}_9 \cdot \mathbb{M}_9 \cdot \mathbb{S}_{9,1} + \mathbf{v}_{15} \cdot \mathbb{M}_{15} \cdot \mathbb{S}_{15,1}] \cdot \mathbb{R}^{\infty}_1. \end{aligned}$$

Other aspects of graph algorithm will be discussed in the respective sections as we examine the modeling problems. Readers interested in seeing the connection between DAG and the matrix inversion of the form $(\mathbb{1} - \mathbb{A})^{-1}$, where $\mathbb{A}$ is substochastic, should take a look at the Appendix.

III. MODELING

The formalism outlined in the previous section shall be applied to simulate long-range diffusion-attachment solid-on-solid growth on a two-dimensional substrate. For simplicity, the underlying lattice structure is simple cubic—though other crystalline structures are of no fundamental difference. Two examples shall be considered: (1) growth on an initially flat substrate and (2) growth around a screw dislocation. For each initial profile of the substrate, graph g, similarly to what is shown in Fig. 1, is constructed where a vertex represents a lattice position and an edge links a pair of adjacent neighbors together. Each vertex contains a number representing the height of the stack of atoms at that site. This implies that overhangs and voids are prohibited. An edge (i,k) contains probability P_{ik} that if an atom is deposited at i, it would move to k. For illustrative purposes, the Wolf-Villain diffusion model is chosen to prescribe such a weight. According to the model [1], an adatom will try to move in such a way that the lateral coordination number is maximized. Should there be more than one such direction, the probability is divided

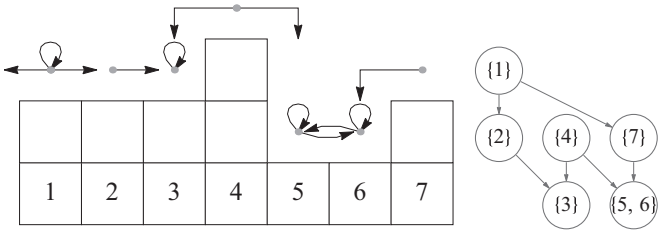

FIG. 3. Diffusion rule for the modified Wolf-Villain model is shown on a sample of a one-dimensional substrate with periodic boundary conditions together with the associated directed acyclic graph. Atoms are deposited from the top and can move at most one step to the side. The arrows depict possible hop directions given the incidence positions. The self-looping arrows designate hopping in-place, which is added in this modified version.

equally among them. A slight alteration is made to the rule by including the coordination number at the present position into consideration so in-place hopping is possible ($P_{ii} \neq 0$). This modification permits the limiting transition probability $\mathbb{R}_s^\infty$ to always exist in our analyses. The underlying graph g of the transition matrix $\mathbb{P}$ serves as the starting point of all of our simulations. We shall examine the surface growth evolution of the examples when each incidence atom, one at a time, performs a random walk on the surface where the direction of each step is given by the modified WV model until the atom becomes a part of the surface. The final resting position of the atom is chosen from one where the atom has visited most frequently.

Before we discuss problem-specific modelings, it is a good idea to consider a simple example. Figure 3 shows the side view of a one-dimensional lattice with periodic boundary conditions at an instant in time. According to our modified Wolf-Villain model, the arrow(s) on top of each surface position indicate possible directions that an atom, if dropped there, would move with the probability inversely proportional to the number of arrows at that point. Lattice positions are labeled by the numbers at the base. The one-step transition matrix is given by

$$\mathbb{P} = \begin{pmatrix} 1/3 & 1/3 & 0 & 0 & 0 & 0 & 1/3 \\ 0 & 0 & 1 & 0 & 0 & 0 & 0 \\ 0 & 0 & 1 & 0 & 0 & 0 & 0 \\ 0 & 0 & 1/2 & 0 & 1/2 & 0 & 0 \\ 0 & 0 & 0 & 0 & 1/2 & 1/2 & 0 \\ 0 & 0 & 0 & 0 & 1/2 & 1/2 & 0 \\ 0 & 0 & 0 & 0 & 0 & 1 & 0 \end{pmatrix}.$$

This example is simple enough that there is no need to cast $\mathbb{P}$ into its canonical form. It is clear from the structure of the matrix that the transient classes are $\{1\},\{2\},\{4\}$, and $\{7\}$ and the recurrent classes are $\{3\}$ and $\{5,6\}$ (which are also our sinks). Since each transient class only contains one member, matrix $\mathbb{M}_s$ is extremely simple; $\mathbb{M}_s = 1/(1 - P_{s,s})$ for $s \in \{1,2,4,7\}$. The recurrent matrices are $\mathbb{R}_1^\infty = \{1\}$ and $\mathbb{R}_{\{5,6\}}^\infty = \left(\begin{smallmatrix} 1/2 & 1/2 \\ 1/2 & 1/2 \end{smallmatrix}\right)$. Matrices $\mathbb{P}_{s,x}^{\text{exit}}$ and $\mathbb{S}_{s,f}^\infty$ can be calculated from Eqs. (8) and (9) with the help of the DAG shown in Fig. 3. For example, given that an atom starts its trip at site 1, the probability $\mathbb{P}_{1,3}^\infty$ that it will end up at site 3 can be computed in the following way:

$$\begin{aligned} \mathbb{P}_{1,3}^\infty = \mathbb{S}_{1,3}^\infty &= \mathbb{P}_{1,2}^{\text{exit}} \cdot \mathbb{M}_2 \cdot \mathbb{P}_{2,3} \cdot \mathbb{R}_3^\infty \\ &= (\mathbb{M}_1 \cdot \mathbb{P}_{1,2}) \cdot \mathbb{M}_2 \cdot \mathbb{P}_{2,3} \cdot \mathbb{R}_3^\infty \\ &= \left(\frac{1}{1-\frac{1}{3}} \times \frac{1}{3}\right) \frac{1}{1-0} \times 1 \times 1 = \frac{1}{2}. \end{aligned}$$

The resulting limiting transition probability matrix for this initial configuration is given by

$$\mathbb{P}^\infty = \begin{pmatrix} 0 & 0 & 1/2 & 0 & 1/4 & 1/4 & 0 \\ 0 & 0 & 1 & 0 & 0 & 0 & 0 \\ 0 & 0 & 1 & 0 & 0 & 0 & 0 \\ 0 & 0 & 1/2 & 0 & 1/4 & 1/4 & 0 \\ 0 & 0 & 0 & 0 & 1/2 & 1/2 & 0 \\ 0 & 0 & 0 & 0 & 1/2 & 1/2 & 0 \\ 0 & 0 & 0 & 0 & 1/2 & 1/2 & 0 \end{pmatrix}.$$

According to $\mathbb{P}^\infty$, an atom falling onto site i will eventually end up at site 3, 5, or 6 with probabilities as listed on the i^{th} row if one applies the modified WV rule repeatedly. Moreover, provided that an atom is likely to fall anywhere, site 3 is the most likely eventual resting place (because the third column of this matrix yields the largest sum) with the probability of $3/7$.

Let us examine the structure of the sinks obtained from the modified WV model in a general two-dimensional substrate. Most of the time, a sink (recurrent) class only contains one member (like site 3 in our simple example above). This member is the representation of a kink site. Thus the task of computing Perron vectors to represent the $\mathbb{R}_s^\infty$ matrices is removed. Essentially, these matrices are simply $\{1\}$. In a few rare cases we could have a situation where two (sites 5 and 6 in the above example), three, or four kinks facing each other create an area of two to four sites whose coordination numbers equal one another and are higher than those of their surrounding neighbors'. Each vertex within a class with two (four) elements has two (three) edges, one pointing to itself and the rest point(s) to its neighbor(s). The limiting recurrent matrix $\mathbb{R}_s^\infty$ in this case would be a 2×2 (4×4) matrix with all elements being $1/2$ ($1/4$). In the case of three elements, there is one vertex with three outgoing edges, while the other two only contain two edges. The Perron vector used in Eq. (4) comprises two of $2/7$ and one of $3/7$. Only in this last case is the weight not distributed evenly and the walker would more likely go there. Fortunately, these cases never crop up in the analyses of the two-dimensional problems considered below.

A. Growth on flat substrate

Here we consider the surface growth on an initially flat rectangular surface with the periodic boundary conditions and apply the algorithm discussed in the previous section to find the most likely site that each atom would likely be. Two different methods shall be used: (I) each deposition site is chosen randomly and the algorithm gives its most probable final position and (II) the most probable final position of all initial sites shall be chosen. Notice that the first atom to be dropped onto the surface will as likely be at any one site as another. Thus, for a visual purpose, we put it at the center of

the surface. This atom will act as the seed to which subsequent atoms can attach themselves in the process of island formation.

In Method I, for each iteration, the simulation scheme starts by randomly selecting a starting position i_0. Then only the subgraph of g whose components can be reached from i_0 is extracted. This process helps keep only the relevant irreducible classes for future computations. Subsequently, the DAG G of this subgraph is constructed by grouping strongly connected components together. We choose the eventual resting position by looking for j which yields the greatest $P^{\infty}_{i_0 j}$. From the structure of G, one of three things could happen: (a) there is only one class thus G is the sink, (b) G only contains one sink and j will inevitably be in that sink, or (c) G contains multiple sinks and further calculation needs to determine the most likely sink that j would eventually lie. It is only this last case that an actual calculation in the form outlined in Sec. II C is performed if all one wishes is to get the final position of the adatom without calculating any statistics. Once all $\mathbf{v}_s, \forall s \in S$ are obtained, the chosen sink is the one whose member has the greatest value among all elements in all sink classes. Should there be more than one such members, the chosen site is selected randomly from that list. We then increment the atomic height at that site by one unit and the whole routine is repeated. Method II is similar to Method I except for one important point; our initial probability distribution $\mathbf{v}_i$ is given by $(1/N)\{1, \ldots, 1\}$ instead of having one nonzero element at a random position i_0.

B. Growth around a screw dislocation

In modeling the surface growth around a screw dislocation, we decide upon a circularly shaped substrate of radius r with free boundary. This choice ensures that any rectangular pattern that might emerge from the growth is due to the underlying lattice structure and not due to the shape of the boundary. Sites along the rim of the disk only connect with those within; thus they contain fewer nearest neighbors than the ones within the disk. The total number of lattice positions is approximately πr^2. We first initialize the height of all lattice points according to $h(x,y) = (b/2\pi)\tan^{-1}(y/x)$. Traversing around the dislocation core at (0,0) once in the clockwise (counterclockwise) direction will result in a height increment (decrement) approaching b at large distance from the core. In order to specify the coordination number at each point on the lattice, one needs to specify the criterion for height difference between any adjacent sites. If the height difference between two nearest-neighboring sites is smaller than $0.2b$, we consider them as living on the same plane, and an adatom on top of the shorter site will not receive the coordination number count from the taller one. The simulation procedures in this case are the same as that of the flat surface. After the most probable site is found in either Method I or Method II, we increase its height by b to match the magnitude of the Burgers vector. Then the process is repeated.

IV. RESULTS AND DISCUSSIONS

The evolution in the case of growth on a flat substrate gives rise to one-island formation. In Method I, subsequent atoms attach themselves to the initial single-atom island since this is the only place where they can maximize their coordination number. The most probable final position of each newly deposited atom given by our algorithm tends to be the kink site that is closest to the dropped position. This results in an island surface with jagged island boundary as shown in Fig. 4(a). The island will continue to grow until the first layer is completely filled up. This happens because there is no mechanism, e.g., Ehrlich-Schwoebel-like barrier, to prevent an adatom dropped on top of the island from hopping down to a lower layer where it could increase its coordination number. After the complete first layer is filled, the growth process repeats itself again and again, giving us a perfect layer-by-layer growth.

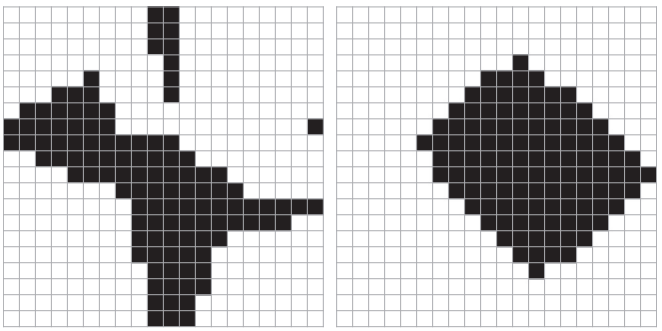

FIG. 4. Surface of size 20×20 lattice sites with periodic boundary conditions after 113 atoms (black squares) are deposited using (a) Method I and (b) Method II.

In Method II, the growth of the freshly deposited layer is largely symmetrical. Identifying the plane of the substrate to be (001), atoms collectively tend to form an island whose boundaries grow outward in a rectangular fashion with growth fronts perpendicular to the [110], [$1\bar{1}0$], [$\bar{1}10$], and [$\bar{1}\bar{1}0$] directions as can be seen in Fig. 4(b). Unlike the previous case, the shape of the island is generally very compact. The development of the growth fronts can be observed since the early stage in the simulation. These orientations are favorable to incoming adatoms than others since they provide more lateral kink sites which result in higher coordination numbers than if the front were one of [100], [010], [$\bar{1}00$], or [$0\bar{1}0$]. As in the previous method, the surface is filled up one layer at a time.

The simulation result of the surface growth around a screw dislocation shows a more interesting dynamics. We initially align the ridge so it extends radially outward from the dislocation core at (0,0) along the [$0\bar{1}0$] direction. When viewed from the top, the ridge starts spiraling outward in the clockwise direction (since the atomic height difference is $h(x = 0^+) - h(x = 0^-) = +b$ along the ridge) as more and more atoms are attracted toward its left side. The surface evolution according to Method I, like the flat substrate case, gives a very rough spiral ridge. The randomness of each deposition causes the atomic incorporation to occur at the nearest kink site which may be anywhere. This makes it difficult to describe how the surface grows generally. More importantly, the growth does not reflect the shape observed in actual experiments where the spiral ridge fronts are of well-defined compact geometrical form [7].

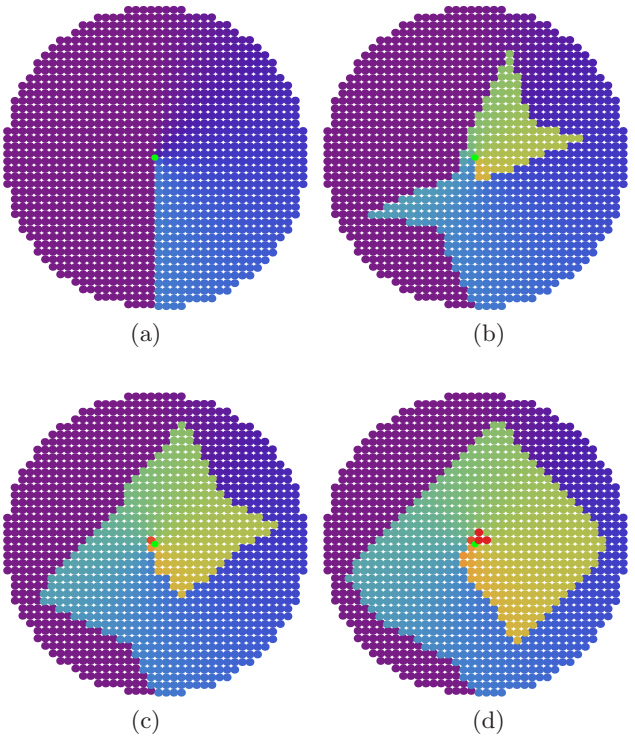

FIG. 5. (Color online) Growth around a screw dislocation starting from (a) initial profile and then after (b) 200 atoms, (c) 400 atoms, and (d) 600 atoms are deposited.

The result from Method II, on the other hand, does not suffer from this setback. During its first revolution, whose development is depicted in Figs. 5(b) and 5(c), the spiral ridge looks like a four-pointed star whose boundary is concave. These concave fronts are filled up quickly afterward into straight edges orienting along the preferred directions, making the spiral rectangular in appearance. The growth fonts are exactly the same as those seen in the case of flat substrate growth. As time progresses, more and more steps are generated and the surface looks like a rectangular pyramid. The distance between adjacent steps also decreases with time, as is typical seen in actual growth experiment [8,26] and also in the phase-field simulation [27]. With this particular boundary condition, we observe the stationary state when the width of successive steps is exactly 1. Since the details of the growth evolution depend largely on the chosen diffusion rule (the modified WV in this case) and the boundary conditions, we shall postpone the full analyses of the dependence of surface growth on these choices for our future work.

It should be mentioned that the strange initial "side-branching" spiral has never been observed elsewhere, either in the phase-field modeling or in energetic-based kMC simulations of growth around a dislocation. We believe that this artifact is specific to our choice of diffusion rule. The shape, however, is similar to a two-dimensional kMC growth simulation around a nucleation site with atoms having a short average mean free path [12]. By employing a multiple registration scheme, the island boundary was smoothed out and the dendritic feature with four side branches could be seen. We believe that their striking resemblance albeit different

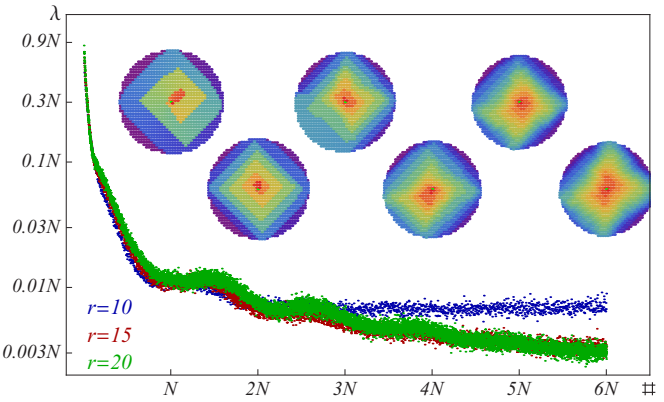

FIG. 6. (Color online) The average mean free path λ simulated by Method I and measured in the units of the respected number of sites N is plot as a function of subsequent drops up to the $6N^{\text{th}}$ atom for circular substrate of radius 10, 15, and 20 as shown in blue (black), red (dark gray), and green (light gray), respectively. The surface profile after every N^{th} deposited atoms simulated by Method II are shown as points of reference.

physical processes may not be a coincidence but an implication about a connection between our probabilistic approach and the approach using short-distance diffusion with a multiple registration scheme.[4] As a noise reduction technique, the scheme allows for a more probable site to be chosen since an atom must visit a site repeatedly up to a certain number before it becomes a part of the surface. Thus, to some degree, the two approaches are similar. Further investigation is needed in order to quantify this connection.

As a demonstration of our probabilistic approach, Fig. 6 shows the mean free path λ, or the average number of hops an atom makes until its incorporation to the most likely spot on the spiral ridge, computed through Method I. The simulations were performed on the substrate of radius $r = 10$, 15, and 20 atomic spacings, bringing the total number of sites to $N = 316$, 716, and 1264, respectively. About $6N$ atoms were sequentially dropped in each case. Points on the graph are the results of the average over 800, 400, and 300 runs respectively. All three graphs are more or less on top of one another except for the tail of the $r = 10$ case. Due to its small size, the system reaches its stationary state long before the other two cases. The very first atom has to hop on the order of $N \sim r^2$ before it reaches the dislocation ridge. The number of hops decreases very rapidly as the ridge starts to spiral. We notice a series of plateaus starting approximately at every N^{th} atoms. A drop in the number of hops to the next plateau occurs as one or more of the ridge fronts are filled up and straightened out. Inside a plateau region, new atoms take on average the same number of hops before reaching the spiral as its fronts propagate outward. This process continues until the stationary state is reached at which point atoms most likely would take at most a few hops before being incorporated into the spiral ridge. As points of

[4]The latter was recently shown to be equivalent and could provide an alternative approach to simulating collective diffusion phenomenon on thin-film growth [28].

reference, we include the shapes of the substrate, simulated by Method II, after N^{th}, $2N^{\text{th}}$, ..., $6N^{\text{th}}$ atoms are absorbed into the spiral.

A few remarks are in order before we end this section. In principle, it is possible to obtain Fig. 6 using the conventional approach by directly applying the WV diffusion rule to each step until an atom no longer moves, while recording its hop number. Doing so repeatedly in order to achieve the same statistics presented here, however, would be computationally very costly. We were able to produce the data used to create the above graphs using about four days of computer time on a single core processor. If one is not interested in carrying out any statistical computations and only wants the evolution of the height profile, a much larger system can be simulated within a reasonable time. As mentioned earlier, in most cases the eventual resting site for each deposited atom may be obtained with minimal computation by simply looking at the structure of the underlying DAG. Finally, the technique presented in this work deals primarily with statistics of random walk on lattices given a local diffusion rule. Readers interested in practical tools for simulating thin film growth on an actual physical system should look into many recent developments aimed toward improving efficiency and accuracy of the conventional kMC algorithm. Amar *et al*. make use of clever parallel programming techniques to extend kMC over larger length and time scales [29] and are able to achieve simulation time that scales as, not the usual polynomial, but the logarithm of system size [30]. For a smaller system that demands full trajectories of deposited atoms, molecular dynamics (MD) is generally utilized. Several accelerated dynamics algorithms have been proposed to speed up direct integrations of Newton's equations, more notably using temperature-accelerated MD technique [31]. Other attempts such as one that tries to approximate the MD methods to be used in conjunction with kMC calculations have also shown impressive speed improvement on long-time/large-scale systems over the conventional kMC approach [32]. Readers wishing to see theoretical basis submolonolayer growth kinetics and follow recent developments in cluster growth on surfaces should consult Ref. [33] and references therein.

V. CONCLUSION

Based on the Markovian hypothesis and Froebenius theorem, the limiting probability transition matrix for a random walker starting a trip with a given initial probability profile is obtained. We devised graph algorithms to automate the process so it could be implemented on a computer. In the process, we discovered an algorithm for finding the inverse of a certain class of stochastic matrices. Finally, the formalism is applied to solid-on-solid, diffusion-attachment type of surface growth on a two-dimensional flat substrate and around a screw dislocation. The latter gives a usual spiral ridge with a rectangular shape reflecting the underlying crystal structure in the limit where atoms are set to emerge at the most probable lattice positions during growth. The result also suggests an interesting connection with the widely used multiple registration technique in kMC simulations.

ACKNOWLEDGMENTS

The author is grateful to Udomsilp Pinsook for his insightful input and valuable suggestions. Fundings from the Faculty of Science, the Special Task Force for Activating Research (STAR), Ratchadaphiseksomphot Endowment Fund Chulalongkorn University through the Energy Materials Physics Research Group, and Thailand Research Fund Grant No. MRG5580245 are acknowledged.

APPENDIX: DAG AND MATRIX INVERSION

An algorithm such as that of Tarjan's which casts a matrix into the corresponding directed acyclic graph from where permutation matrix $\mathbb{Q}$ could be constructed offers a new way of computing an inverse of a certain class of matrix. It is well known that the inverse of a triangular block matrix is given by

$$\begin{pmatrix} \mathbb{B}_1 & \mathbb{B}_2 \\ \mathbb{O} & \mathbb{B}_3 \end{pmatrix}^{-1} = \begin{pmatrix} \mathbb{B}_1^{-1} & -\mathbb{B}_1^{-1}\cdot\mathbb{B}_2\cdot\mathbb{B}_3^{-1} \\ \mathbb{O} & \mathbb{B}_3^{-1} \end{pmatrix}. \tag{A1}$$

We shall use Eq. (A1) as a basis for our analysis.

We are interested in finding the inverse of matrix $\mathbb{D} \equiv \mathbb{1} - \mathbb{A}$, where $\mathbb{A}$ is a substochastic matrix whose summation of elements in each row is less than or equal to 1. We start by obtaining $\mathbb{Q}$ through Tarjan's algorithm. Matrix $\mathbb{Q}$ can be used to turn $\mathbb{A}$, through a simple change of basis, into

$$\widetilde{\mathbb{A}} \equiv \mathbb{Q}^{\top}\cdot\mathbb{A}\cdot\mathbb{Q} = \begin{pmatrix} \mathbb{T}_1 & \mathbb{T}_{1,2} & \cdots & \mathbb{T}_{1,t} \\ \mathbb{O} & \mathbb{T}_2 & \cdots & \mathbb{T}_{2,t} \\ \vdots & \ddots & \ddots & \vdots \\ \mathbb{O} & \cdots & \mathbb{O} & \mathbb{T}_t \end{pmatrix}.$$

Matrix $\widetilde{\mathbb{A}}$ would have the same structure as, e.g., $\widetilde{\mathbb{P}}_{\mathcal{T}\to\mathcal{T}}$ shown in Eq. (3), where each $\mathbb{T}_i$ and $\mathbb{T}_{i,j}$ are irreducible. Figure 7 gives an example of the underlying DAG of $\widetilde{\mathbb{A}}$ for $t = 6$, assuming that all of the upper triangular block matrices are nonzero.

Let $\mathbb{M}_i \equiv (\mathbb{1} - \mathbb{T}_i)^{-1}$ and $S(i,j)$ be the set of all possible subsets of $\{i, i+1, \ldots, j\}$ with i and j as the first and the last elements and listed in increasing order; for example, $S(1,4) = \{\{1,2,3,4\},\{1,2,4\},\{1,3,4\},\{1,4\}\}$. One can recursively apply

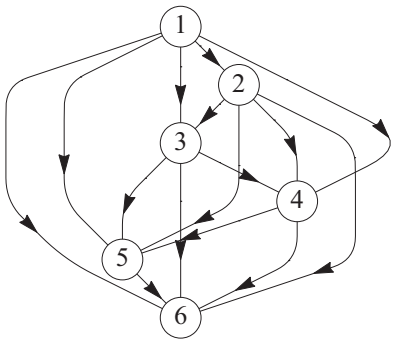

FIG. 7. An example of a directed acyclic graph representing a matrix in its canonical form.

Eq. (A1) to compute the inverse of

$$\widetilde{\mathbb{D}} = \mathbb{1} - \widetilde{\mathbb{A}} = \begin{pmatrix} \mathbb{1}-\mathbb{T}_1 & -\mathbb{T}_{1,2} & \cdots & -\mathbb{T}_{1,t} \\ \mathbb{O} & \mathbb{1}-\mathbb{T}_2 & \cdots & -\mathbb{T}_{2,t} \\ \vdots & \ddots & \ddots & \vdots \\ \mathbb{O} & \cdots & \mathbb{O} & \mathbb{1}-\mathbb{T}_t \end{pmatrix}. \quad \text{(A2)}$$

It is straightforward to show that the $(i,j)^{\text{th}}$ block component of $\widetilde{\mathbb{D}}^{-1}$ is given by

$$[\widetilde{\mathbb{D}}^{-1}]_{i,j} = \begin{cases} \mathbb{M}_i & i = j, \\ \mathbb{M}_i \cdot \sum_{s \in S(i,j)} \prod_{k=1}^{\|s\|-1} (\mathbb{T}_{s_k,s_{k+1}} \cdot \mathbb{M}_{s_{k+1}}) & i < j, \\ \mathbb{O} & i > j. \end{cases} \quad \text{(A3)}$$

The sum in the case of $i < j$ is taken over all members s of $S(i,j)$, where s_k denotes the k^{th} element of s and $\| s \|$ denotes the number of elements. Once the inverses of all block elements are computed and the whole $\widetilde{\mathbb{D}}^{-1}$ is assembled, one can simply perform another change of basis to shuffle all elements back to their original orders.

Equation (A3) may be conveniently read off from the structure of the DAG of $\widetilde{\mathbb{A}}$. To obtain the $(i,j)^{\text{th}}$ block component, one simply traverses the graph from node i to j through all possible routes. Each visit to node k corresponds with $\mathbb{M}_k$. Each passage through an edge from l to m corresponds with $\mathbb{T}_{l,m}$. The final result is the sum over these routes. This method amounts to graph traversal, which is a common routine in graph programming.

Our method of finding an inverse not only is simple but also reveals the fundamental structure of the matrix. Moreover, in some problems, only a small subset of inverse matrix elements are needed. Our method would tremendously reduce the amount of computation because only a few $\mathbb{M}_i$'s may be required. Finally, we should point out that directly finding $\mathbb{A}^{-1}$ is not much harder than finding $\mathbb{D}^{-1}$. The additional difficulty arises in keeping track of extra minus signs that crops up depending on whether the number of $\mathbb{T}_{l,m}$'s in an expression is odd or even. This could be done simply by counting the number of nodes visited during the traversal.

[1] D. E. Wolf and J. Villain, Europhys. Lett. **13**, 389 (1990).

[2] S. Das Sarma and P. I. Tamborenea, Phys. Rev. Lett. **66**, 325 (1991).

[3] S. Das Sarma, C. J. Lanczycki, R. Kotlyar, and S. V. Ghaisas, Phys. Rev. E **53**, 359 (1996); P. I. Tamborenea and S. Das Sarma, *ibid.* **48**, 2575 (1993).

[4] G. Palasantzas and J. Krim, Phys. Rev. Lett. **73**, 3564 (1994).

[5] M. E. J. Newman, *Networks: An Introduction* (Oxford University Press, New York, 2010); S. H. Strogatz, Nature **410**, 268 (2001); R. Albert and A.-L. Barabási, Rev. Mod. Phys. **74**, 47 (2002); S. Boccaletti, V. Latora, Y. Moreno, M. Chavez, and D. Hwang, Phys. Rep. **424**, 175 (2006).

[6] See, for example, L. Lovász, in *Combinatorics: Paul Erdos Is Eighty*, Vol. 2, edited by D. Miklos, V. T. Sos, and T. Szonyi (Bolyai Society Mathematical Studies, Budapest, 1993), pp. 1–46; F. R. K. Chung, *Spectral Graph Theory*, CBMS Regional Conference Series in Mathematics No. 92 (American Mathematical Society, Rhode Island, 1997).

[7] B. Heying, E. J. Tarsa, C. R. Elsass, P. Fini, S. P. DenBaars, and J. S. Speck, J. Appl. Phys. **85**, 6470 (1999); A. Parkhomovsky, A. M. Dabiran, B. Benjaminsson, and P. I. Cohen, Appl. Phys. Lett. **78**, 2315 (2001); Y. Cui and L. Li, Phys. Rev. B **66**, 155330 (2002).

[8] G. Springholz, A. Y. Ueta, N. Frank, and G. Bauer, Appl. Phys. Lett. **69**, 2822 (1996).

[9] S. A. Morin and S. Jin, Nano Lett. **10**, 3459 (2010).

[10] W. K. Burton, N. Cabrera, and F. C. Frank, Philos. Trans. R. Soc. (London) A **243**, 299 (1951); N. Cabrera and M. M. Levine, Philos. Mag. **1**, 450 (1956).

[11] A. Redinger, O. Ricken, P. Kuhn, A. Rätz, A. Voigt, J. Krug, and T. Michely, Phys. Rev. Lett. **100**, 035506 (2008); Y. M. Yu, B. G. Liu, and A. Voigt, Phys. Rev. B **79**, 235317 (2009).

[12] R.-F. Xiao, D. Alexander, and F. Rosenberger, J. Cryst. Growth **109**, 43 (1991); R.-F. Xiao, J. I. Alexander, and F. Rosenberger, Phys. Rev. A **43**, 2977 (1991).

[13] R.-F. Xiao, J. I. Alexander, and F. Rosenberger, Phys. Rev. A **38**, 2447 (1988); C. Tang, *ibid.* **31**, 1977 (1985).

[14] G. Antczak and G. Ehrlich, J. Chem. Phys. **129**, 124702 (2008).

[15] S. C. Wang, J. D. Wrigley, and G. Ehrlich, J. Chem. Phys. **91**, 5087 (1989).

[16] G. Antczak and G. Ehrlich, Surf. Sci. Rep. **62**, 39 (2007); S.-M. Oh, S. J. Koh, K. Kyuno, and G. Ehrlich, Phys. Rev. Lett. **88**, 236102 (2002); T. R. Linderoth, S. Horch, E. Lægsgaard, I. Stensgaard, and F. Besenbacher, *ibid.* **78**, 4978 (1997);

[17] K. Oura, V. G. Lifshits, A. A. Saranin, A. V. Zotov, and M. Katayama, *Surface Science: An Introduction* (Springer-Verlag, Berlin, Germany, 2003), Chap. 13.

[18] G. R. Grimmett and D. R. Stirzaker, *Probability and Random Processes*, 2nd ed. (Oxford University Press, New York, 1992).

[19] For rigorous proofs, please consult, e.g., C. D. Meyer, *Matrix Analysis and Applied Linear Algebra* (SIAM, Philadelphia, 2000).

[20] O. Perron, Math. Ann. **64**, 248 (1907); G. Frobenius, Sitzungsber. Königl. Preuss. Akad. Wiss. Berlin, 456 (1912).

[21] A. Berman and R. J. Plemmons, *Nonnegative Matrices in the Mathematical Sciences* (SIAM, Philadelphia, 1994).

[22] B. Aspvall, M. F. Plass, and R. E. Tarjan, Inform. Process. Lett. **8**, 121 (1979); T. H. Cormen, C. E. Leiserson, R. L. Rivest, and C. Stein, *Introduction to Algorithms* (MIT Press and McGraw-Hill, New York, 2001), pp. 552–557, 2nd ed.

[23] A. B. Kahn, Commun. ACM **5**, 558 (1962); R. E. Tarjan, Acta Informatica **6**, 171 (1976).

[24] J. P. Jarvis and D. R. Shier, in *Applied Mathematical Modeling: A Multidisciplinary Approach*, edited by D. R. Shier and K. T. Wallenius (CRC Press, Boca Raton, FL, 1999), pp. 271–289, Chap. 13.

[25] R. S. Varga, *Matrix Iterative Analysis*, 2nd ed. (Springer-Verlag, New York, 2000).

[26] C. Gerber, D. Anselmetti, J. G. Bednorz, J. Mannhart, and D. G. Schlom, Nature **350**, 279 (1991).

[27] A. Karma and M. Plapp, Phys. Rev. Lett. **81**, 4444 (1998).
[28] F. D. A. Aarão Reis, Phys. Rev. E **81**, 041605 (2010).
[29] Y. Shim and J. G. Amar, Phys. Rev. B **71**, 125432 (2005).
[30] Y. Shim, J. G. Amar, B. P. Uberuaga, and A. F. Voter, Phys. Rev. B **76**, 205439 (2007).
[31] Y. Shim and J. G. Amar, J. Chem. Phys. **134**, 054127 (2011).
[32] G. Grochola, I. K. Snook, and S. P. Russo, Phys. Rev. B **84**, 165442 (2011).
[33] M. Einax, W. Dieterich, and P. Maass, Rev. Mod. Phys. **85**, 921 (2013).